New Products from the Heptalene-Forming Reaction of Azulenes and Acetylenedicarboxylates in Polar Media

by **Gurmit Singh**, **Anthony Linden**, **Khaled Abou-Hadeed**, and **Hans-Jürgen Hansen***

Organisch-chemisches Institut der Universität Zürich, Winterthurerstrasse 190, CH-8057 Zürich

A number of azulenes **1**, in particular those with π-substituents at C(6) such as phenyl, 3,5-dimethylphenyl, and 4-biphenyl, have been reacted with 3 mol-equiv. of dimethyl acetylenedicarboxylate (ADM) in MeCN at 110° (*cf. Scheme 1*). Main products had been, in all cases, the corresponding heptalene-4,5-dicarboxylates **2**. However, a whole number of side products, mainly rearranged (1 + 2)-adducts with two molecules of ADM, in amounts of 0.2–9% were also isolated and characterized (*cf. Scheme 2*). The 2a,8a-dihydro-3,4-ethenoazulene-1,2-dicarboxylates **14**, formed by energetically favorable ring closure from the solvent-stabilized zwitterions **15**, resulting from bond heterolysis in the primary cycloadducts **12** (*cf. Scheme 3*), have been mechanistically identified as the pivotal intermediates responsible for the formation of all side product (*cf. Schemes 5*, *9*, *12*, and *13*). Deuterium-labeling experiments were in agreement with the proposed mechanisms, indicating that sigmatropic [1,5s]-H shifts in **14** (*cf. Scheme 6*) as well as isoconjugate [1,4s]-H shifts in resonance-stabilized zwitterions of type **21** (*cf. Scheme 9*) are the crucial steps for side-product formation. It is postulated that a concluding antarafacial 8e-dyotropic rearrangement is responsible for the appearance of the 2,4a-dihydrophenanthrene-tetracarboxylates of type *trans*-**6** (*cf. Scheme 9*) in the reaction mixtures, which further rearrange thermally by a not fully understood mechanism into the isomeric tetracarboxylates **7** (*cf. Schemes 10* and *11*). Most surprising is the presence of a small amount (0.3–1%) of the azulene-4,5,7,8-tetracarboxylate **9** in the reaction mixture of azulene **1a** and ADM. It is proposed that the formation of **9** is the result of a [1,5s]-C shift in the spiro-linked intermediates **24**, which, after prototropic shift and take-up of a third molecule of ADM, disintegrate by a retro-*Diels-Alder* reaction into **9** and the phthalic diesters **30** (*cf. Scheme 12*). The UV/VIS spectra of the π-substituted heptalene-4,5-dicarboxylates **2d**–**2f** and their double-bond shifted (DBS) forms **2d**–**2f** (*cf. Table 4* and *Figs. 9–12*) exhibit in comparison with the heptalene-dicarboxylates **2a** and **2′a**, carrying a *t*-Bu group at C(8), only marginal differences, which are mainly found in the relative intensity and position of heptalene bands **II** and **III**.

1. Introduction. – There are good evidences that the formation of heptalene-4,5-dicarboxylates from azulenes and acetylenedicarboxylates (ADR) in apolar media such as tetralin [1], decalin [2], or toluene [3] takes place *via* the intermediate 1,3a-dihydro-1,3a-ethenoazulene-9,10-dicarboxylates, which are generated in a *Diels-Alder*-type reaction of ADR to the five-membered ring of the azulenes (*cf.* [2][4]). These primary adducts rearrange to the observed heptalene-4,5-dicarboxylates (*cf.* [5]). The transformations originally performed by *Hafner et al.* [1] at temperatures >190° are best conducted in toluene at 110–130°, where the yields of the heptalene-4,5-dicarboxylates are the highest since side-product formation is distinctly reduced (*cf.* [3][6]).

In the course of our investigations concerning the influence of π-substituents at the heptalene core on UV/VIS spectra of heptalene-4,5-dicarboxylates and their double-bond-shifted (DBS) isomers, the heptalene-1,2-dicarboxylates (*cf.* [3a][7][8]), we were interested in the synthesis of 8-aryl-substituted heptalene-4,5-dicarboxylates, starting with the corresponding 6-aryl-substituted azulenes. Taking into account that

azulenes with Me substituents at C(1) and C(4) give always the highest yields of the corresponding heptalene-4,5-dicarboxylates (*cf.* [1–3][9]), we chose the 6-aryl-1,4,8-trimethylazulenes **1d**–**1f**[1]) and dimethyl acetylenedicarboxylate (ADM) as starting materials and later included in our investigations the corresponding 6-(*t*-Bu) and 6-Me derivatives **1a** and **1b**, respectively, as well as guaiazulene (**1c**; *Scheme 1*).

Scheme 1

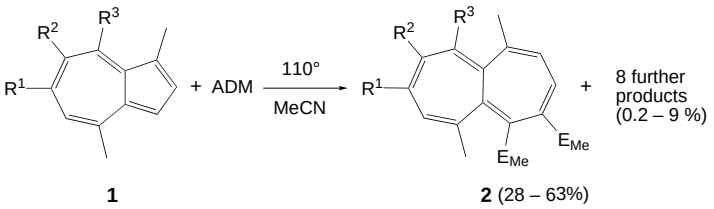

1 **2** (28 – 63%)

a R^1 = *t*-Bu, R^2 = H, R^3 = Me; **b** R^1 = R^3 = Me, R^2 = H;
c R^1 = R^3 = H, R^2 = i-Pr; **d** R^1 = Ph, R^2 = H, R^3 = Me;
e R^1 = 3,5-$Me_2C_6H_3$, R^2 = H, R^3 = Me[a]); **f** R^1 = 4-PhC_6H_4, R^2 = H, R^3 = Me;
E_{Me} = COOMe

[a]) The thermal reaction of **1e** and ADM was only performed in toluene.

For the thermal transformations, we used MeCN as a polar aprotic solvent, which allowed us to work at 110°. The heptalene-4,5-dicarboxylates **2** were the main products in all transformations; however, in addition, a whole number of unexpected adducts, formed from one molecule of azulene and two molecules of ADM, were also isolated. The structure of these products and reflections on the mechanisms of their formation will be discussed in the following parts.

2. Results and Discussion. – The thermal reactions of the azulenes **1** were, with one exception, performed in 0.3M solutions of dry MeCN with 3 mol-equiv. of ADM at 110° during 24 h. The products were isolated by column chromatography (silica gel; hexane/Et_2O mixtures). Additional HPLC separations were necessary in some cases. The product mixtures were not always separated, but rather identified by their specific H-shifts in the corresponding ^{1}H-NMR spectra, based on fully characterized compounds. They were also identified by their characteristic UV/VIS spectra, by their typical R_f or t_R values, or by GC/MS analyses. The combined and complete product pattern that has been elucidated for the reactions of **1** with ADM in MeCN is displayed in *Scheme 2*.

We have already demonstrated (*cf.* [2][4–6]) that there are three reaction channels *I*–*III* for the interaction of azulenes **1** and ADM (*Scheme 3*). Under normal thermal and structural conditions (see below), only paths *I* and *II* are entered, whereby path *I* is controlled by the HOMO of azulene and highly reversible due to the comparably small $\Delta\Delta H_f^\circ$ of the reactants and the 1,3a-dihydro-1,3a-ethenoazulene-9,10-dicarboxylates **12** (all ΔH_f° data from AM1 calculations). Path *I* is the normal way by which reactions

[1]) Azulenes substituted at C(4), C(6), and C(8) can easily be prepared, following the procedure of *Hafner* and *Kaiser* [10] (see *Exper. Part*).

Scheme 2

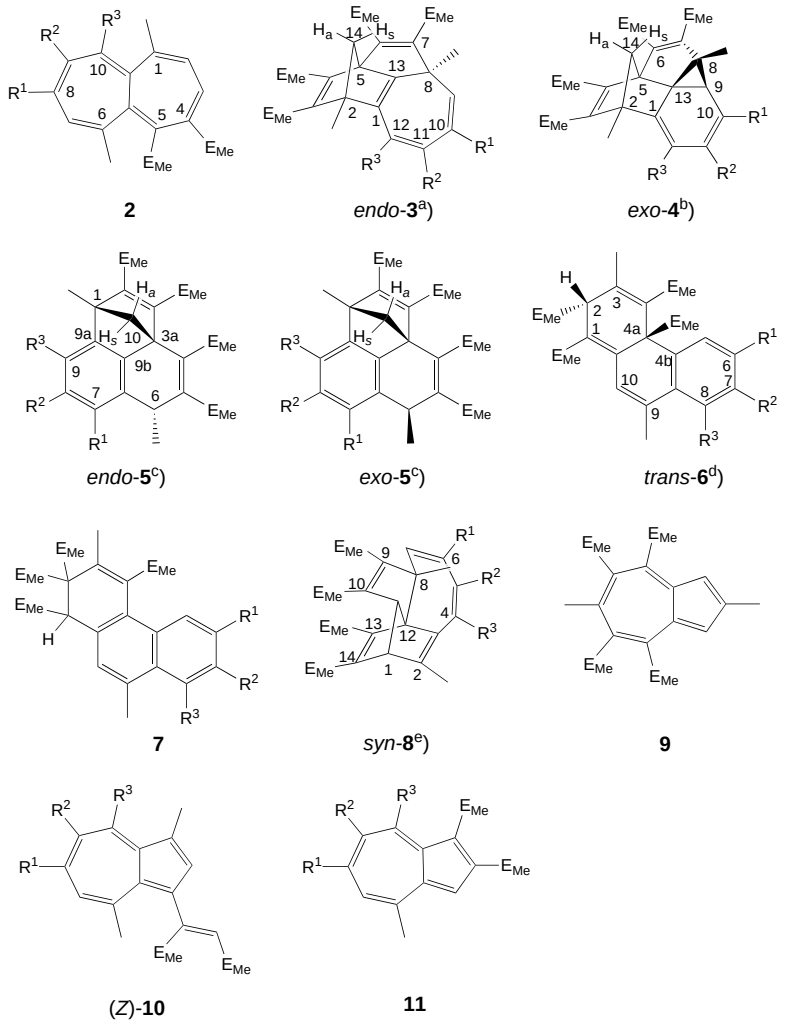

a) *endo* = (2*R**,5*R**,8*S**)- and *exo* = (2*R**,5*R**,8*R**)-diastereoisomer. b) *exo* = (2*R**,5*R**,8*S**, 9*R**,13*R**)- and *endo* = (2*R**,5*R**,8*R**,9*S**,13*S**)-diastereoisomer. c) *exo* = (1*R**,3a*S**,6*R**)- and *endo* = (1*R**,3a*S**,6*S**)-diastereoisomer. d) *trans* = (2*R**,4a*S**)-form. e) *syn* = (1*R**,8*S**,11*R**,12*R**)-form.

take place, producing the heptalene-4,5-dicarboxylates **2** [2]. Path *II* is controlled by the SHOMO of azulene and gives rise to the tricyclic compounds **13** [4], which are formed irreversibly under the reaction conditions and may further react with ADM [12]. Path *III*, leading to the *cis*-configured tricyclic compounds **14**, is not available purely thermally, because most azulenes allow no concerted bonding at C(1) and C(8), or at C(3) and C(4), respectively, due to the fact that the HOMO of these azulenes has orbital coefficients at C(4,6,8) that are zero or at least close to zero. Heavily

Scheme 3

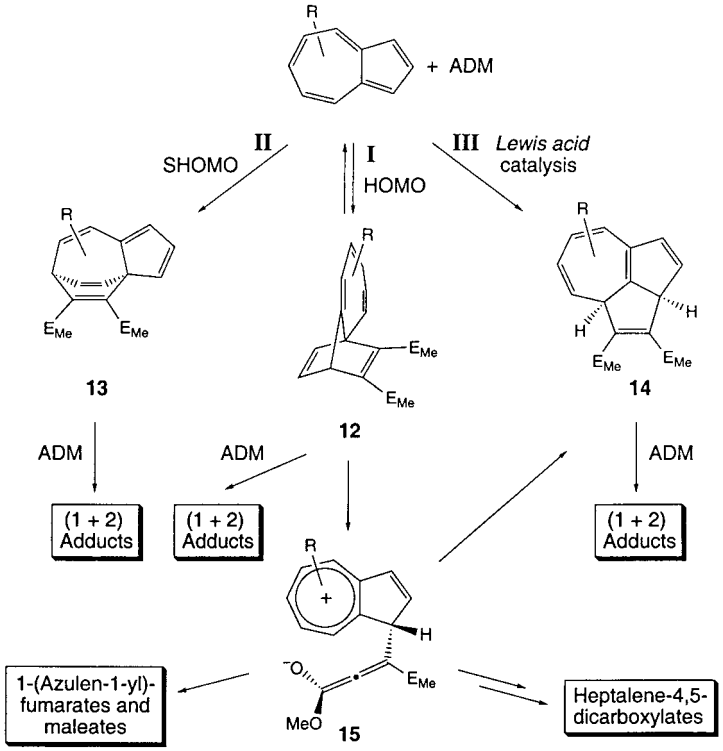

unsymmetrical substitutions patterns of azulenes such as those in benz[*a*]azulenes may change this situation and give rise to the formation of **14** as intermediates [6][13]. However, two-step reactions of azulenes and ADM *via* free zwitterions of type **15** [5], or as given by *Lewis*-acid catalysis, always result in the *cis*-configured intermediates **14** [11], which possess, similarly as the tricycles **13**, large $\Delta\Delta H_f^\circ$ values with respects to the reactants. All of the primary intermediates **12**–**14** are prone to undergo further addition reactions with ADM.

The formation of the heptalenedicarboxylates **2** is always accompanied to a certain extent by azulene-1,2-dicarboxylates **11** (*Scheme 2*) due to a retro-*Diels-Alder* reaction of the primary intermediates **12** under loss of the C(1)=C(2) fragment of the starting azulenes **1**. In this respect, the formation of **11** is a good indicator that the intermediates **12** are indeed formed (*cf.*, *e.g.*, [2][4]). The azulen-1-yl-substituted maleates (*Z*)-**10** and the diastereoisomeric fumarates (*E*)-**10** are generally formed from the corresponding azulenes and ADM in protic solvents (*cf.*, *e.g.*, [5][11]), but may also be generated in small amounts in other solvents. In the present case, it is of interest to note that we could detect only the (*Z*)-isomers. Both, the (*Z*)- and (*E*)-isomers can easily be differentiated by their ^{1}H-NMR spectra, since H–C(2) as well as MeOCO–C(2) show for the (*Z*)- and (*E*)-forms great and inverse shift differences (*cf.* [5][11] and *Exper.*

Table 1. *Characterized Products of Type* **3**, **4**, *and* **5** [a])

Starting azulene [b])	*endo*-**3** [%]	*exo*-**4** [%]	*endo*-**5** [%]	*exo*-**5** [%]
1a	9	0.8	n.o.	n.o.
1b	2	1	n.o.	n.o.
1c	0.5	0.4	0.3	0.4
1d	< 0.3	< 0.3	4	n.o.
1f	n.o.	< 0.3	< 0.3	n.o.

[a]) n.o. = not observed, *i.e.*, no spectroscopic or analytical evidence that the compound was present in amounts > 0.2% in the reaction mixtures. [b]) See *Scheme 1* for substituents.

Part). All the other product types presented in *Scheme 2* are new and, in spite of the somewhat peculiar structures, they have to enter the scene by one of the three primary reaction channels discussed. In the following chapters, we will unfold that they all arise from the corresponding tricyclic intermediates **14**.

2.1. *Structure and Formation of* endo-**3**, exo-**4**, *and* exo- *and* endo-**5**. *Table 1* gives a survey of the isolated and characterized products. The methano-bridge in all three product types indicates the structural and mechanistic relationship of these compounds. Typical in their ^{1}H-NMR spectra is the *AB* signal pattern of the H-atoms at the methano-bridge with J_{AB} in the range of 6–8 Hz as usually observed for norbornadienes and related structures (*cf.*, *e.g.*, [14]). Moreover, H_a and H_s (*Scheme 2*) are clearly distinguished by their chemical shifts. The H_a-atoms are located above the MeOCO-substituted etheno-bridge and appear at much lower field, in the range of 2.9–2.6 ppm ($CDCl_3$) than their geminal *syn*-counterparts (2.4–1.9 ppm). The assignment of the signals is unequivocal, since only the H_s-atom shows the expected $^4J(^1H,^{13}C)$ *W*-coupling with the ester-carbonyl C-atoms at C(3) and C(4) (*cf.* **3** and **4**), or C(2) and C(3) (*cf.* **5**). The structure of both *exo*-**4a** and *endo*-**5d** was further established by X-ray crystal-structure analysis (*Figs. 1* and *2*). The crystals of *endo*-**3a** were of insufficient quality X-ray crystal-structure analysis. However, the complete lack of an NOE effect between H_s–C(14) and Me–C(8) is compatible with only the *endo*-compound. The AM1-calculated structure of this compound is shown in *Fig. 3*[2]).

Some time ago, we reported that the primary intermediates **12** of azulenes **1** (with no substituents at C(4) and C(8)) and ADM are transformed in MeCN at 110° into both corresponding fumarates (*E*)-**10** and the ethano-bridged azulene-1,2-dicarboxylates **16** (*Scheme 4*) [5]. Both types of product must emerge from the corresponding zwitterions **15**, which normally are the source of the heptalene-4,5-dicarboxylates **2**. In these cases, however, the zwitterions **15** are trapped by proton transfer to yield (*E*)-**10** or undergo ring closure to give rise to the tricyclic intermediates **14**, which then tautomerize to **16**. We assume that a similar reaction sequence plays the decisive role

[2]) The AM1-calculated structure of *exo*-**3a** yields an interatomic distance between H_s–C(14) and the closest H-atom of Me–C(8) of 320 pm, whereby the shortest possible distance amounts to 304 pm. In other words, the *exo*-structure of **3a** should exhibit a distinct NOE effect as observed for *exo*-**4a**, in which the corresponding interatomic distance amounts to 306 pm according to its X-ray crystal structure. The AM1-calculated distance of 307 pm speaks clearly for the reliability of the calculated structural data in this series.

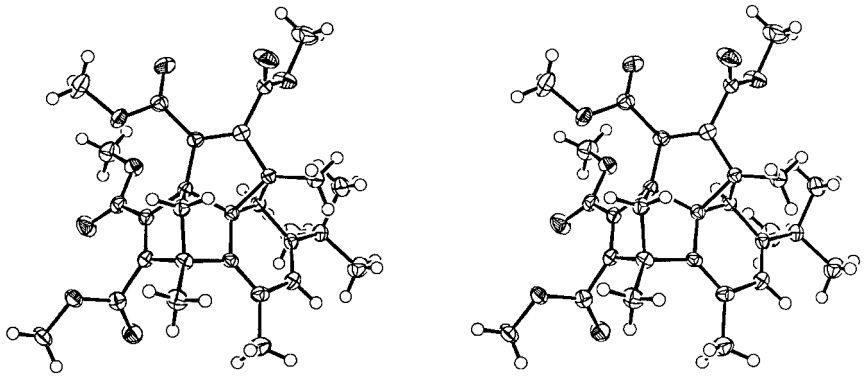

Fig. 1. *Stereoscopic view of the X-ray crystal-structure of tetramethyl* exo-*10-(*tert-*butyl)-2,8,12-trimethylpentacyclo[6.4.1.1*^{2,5}*.0*^{5,13}*.0*^{9,13}*]tetradeca-1(12),3,6,10-tetraene-3,4,6,7-tetracarboxylate* (*exo-***4a**)

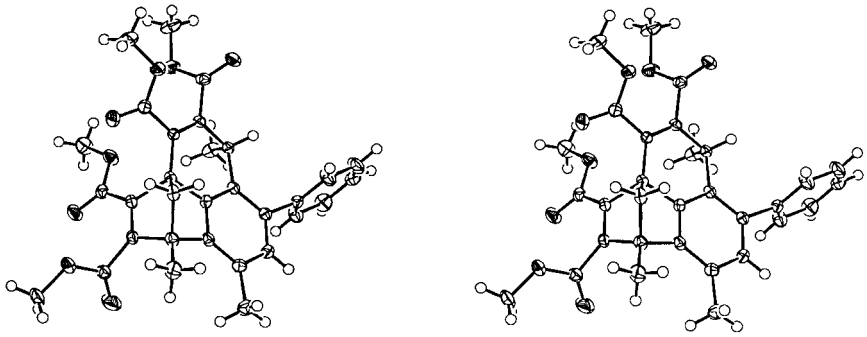

Fig. 2. *Stereoscopic view of the X-ray crystal-structure of tetramethyl* endo-*3a,6-dihydro-1,6,9-trimethyl-7-phenyl-1,3a-methanophenalene-2,3,4,5-tetracarboxylate* (*endo-***5d**)

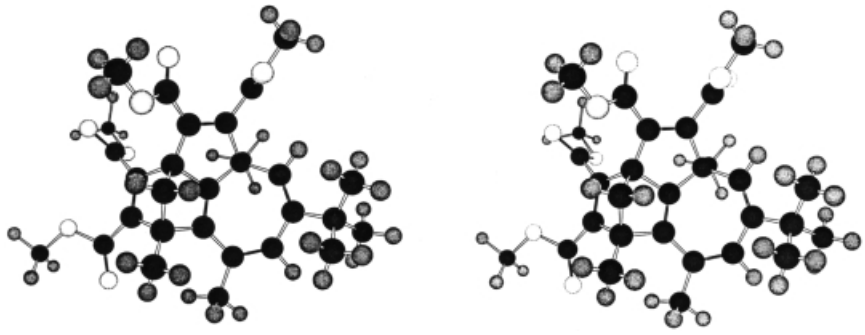

Fig. 3. *Stereoscopic view of the AM1-calculated structure of tetramethyl* endo-*10-(*tert-*butyl)-2,8,12-trimethyltetracyclo[6.4.1.1*^{2,5}*.0*^{5,13}*]tetradeca-1(13),3,6,9,11-pentaene-3,4,6,7-tetracarboxylate* (*endo-***3a**)

Scheme 4

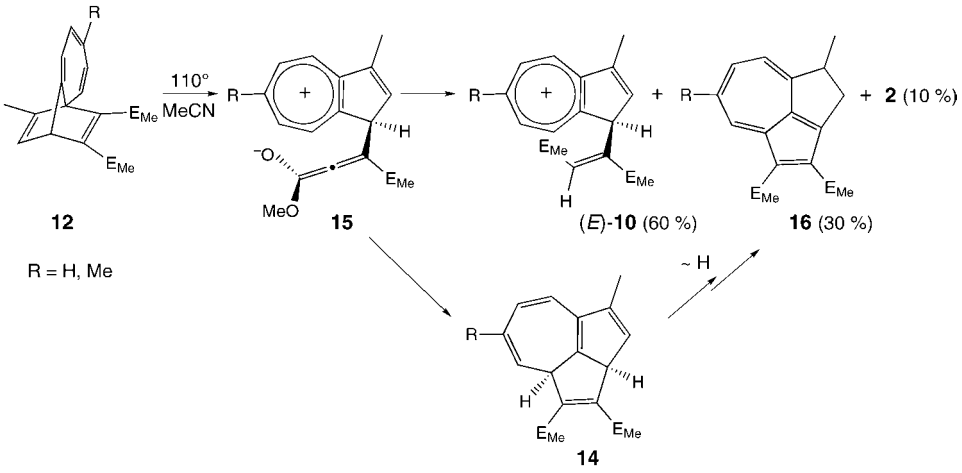

for the appearance of compounds **3**–**5** in the reaction mixtures of the azulenes **1** (*Scheme 5*).

The tricyclic intermediates **14** contain a cyclopentadiene substructure, which should allow reversible sigmatropic [1,5s]-H shifts to give **17**, reactions that take place in cyclopentadiene itself at ambient temperature [15]. The calculated $\Delta\Delta H_f^\circ$ values for the structures **14** and **17** amount to only 0.5 kcal·mol^{-1} in favor of **17**, *i.e.*, the equilibrium mixture at 110° should consist of **14** and **17** in comparable amounts. These are ideal conditions for *Diels-Alder* reactions of **17** with ADM, which may occur in a *syn* or *anti* manner with respect to the Me group at C(8a) of the 3,8a-dihydro-3,4-ethenoazulene skeleton of **17** (*Scheme 5*). This opens the way to the *endo*- and *exo*-configured compounds **3**, **4**, and **5** that have been found in the reaction mixtures of **1** and ADM in MeCN (*cf. Table 1*). The structures of **3**–**5** leave little doubt that these compounds are linked by a reaction sequence that starts with a cycloheptatriene $\rightleftharpoons$ norcaradiene equilibrium that reversibly converts **3** to **4**. The final step seems to be induced by heterolytic cleavage of the C(8)–C(13) bond of the three-membered ring, followed by an energetically favorable [1,2s]-H shift in the zwitterions formed leading to aromatization of the six-membered ring. We have observed this reaction sequence in many other cases (see, *e.g.*, [13]).

Since the tricyclic intermediates **14** have to be *cis*-configured for energetic reasons, there is the possibility to confirm the reaction mechanism postulated (as displayed in *Scheme 5*) by thermal reaction of 3-deuterated **1a** (0.52 [^{2}H] at C(3)) with ADM. The ^{2}H-**14a** formed has to carry the ^{2}H-label at C(2a) in *cis*-relation with respect to Me–C(8) (*Scheme 6*). The *cis*-arrangement will be maintained in the course of the suprafacial ^{2}H migration, which leads to [3-^{2}H]-**17a**. A *syn*-addition of ADM must place the label exclusively at the *anti*-position of C(14) of *endo*-**3a**, whereas an *anti*-addition will lead to the formation of *exo*-[14-^{2}H$_s$]-**3a**, which, on internal ring closure, will result in the formation of *exo*-[14-^{2}H$_s$]-**4a**. Indeed, this is exactly what we observed. Purified *endo*-**3a** displayed in the ^{2}H-NMR spectrum for ^{2}H–C(14), in agreement with

Scheme 5

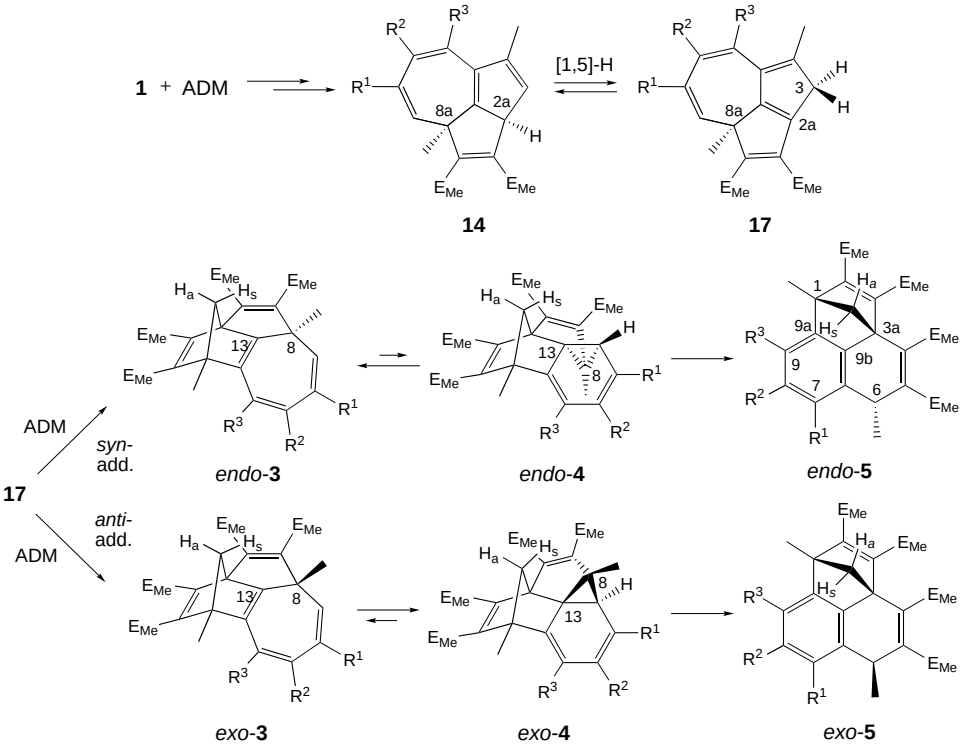

its *anti*-position, only a br. *s* at 2.74 ppm and, in the ^{1}H-NMR spectrum for H–C(14), *s*, integrating for 1.00 H, at 2.28 ppm, indicating the *syn*-position of this H-atom. The reverse was found for labeled *exo*-**4a**. It exhibited in the ^{2}H-NMR spectrum for ^{2}H–C(14) a single br. *s* at 1.88 ppm, indicating its *syn*-position, and in the ^{1}H-NMR spectrum a *s* at 2.64 ppm for H_a–C(14) (integrating again for 1.00 H).

Control experiments with *endo*-**3a** and *exo*-**4a** showed that both compounds were stable under the reaction conditions. Moreover, heating both compounds in DMF at 150° (*cf.* [13]) led neither to *endo*-**5a** nor to *exo*-**5a**, respectively, in analogy to the formation of *endo*-**5c** and *exo*-**5c** (*cf. Table 1*). Over longer heating periods, both *endo*-**3a** and *exo*-**4a** were destroyed. The thermal reaction of **1b** and ADM gave similar results as with **1a**. It seems, therefore, that both *endo*-**3a** and *endo*-**3b**, and *exo*-**4a** and *exo*-**4b** are 'dead ends' under these reaction conditions. It means that the postulated cycloheptatriene $\rightleftharpoons$ norcaradiene equilibrium lies for the *endo*-series mostly on the side of the tetracyclic compounds **3** and in the *exo*-series for the most part on the side of pentacyclic forms **4**. These assumptions are in agreement with the AM1-calculated $\Delta\Delta H_f^\circ$ values of **3**, **4**, and **5** in the *endo*- and *exo*-series (*cf. Table 2*). The data clearly demonstrate that the formation of *endo*-**3** and *exo*-**3** should take place, since $\Delta\Delta H_f^\circ$ (*endo*-**3**–*exo*-**3**) amounts to an average value of -5.0 kcal·mol^{-1}, in agreement with the general observation that more *endo*-**3a** than *exo*-**3a** (in form of its follow-up product

Scheme 6

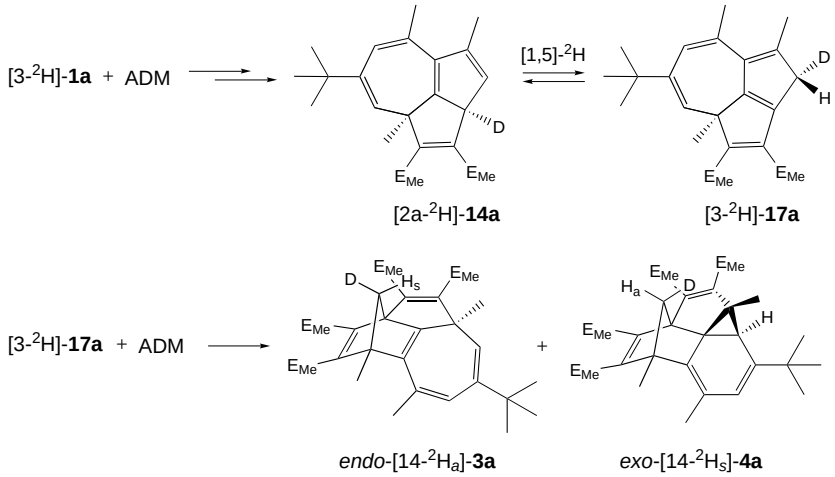

exo-**4a**) was found in the reaction mixtures of **1a** and ADM. However, the next step, *i.e.,* the formation of the norcaradiene substructure of **4**, exhibits great differences in $\Delta\Delta H_f^\circ$ (**4** – **3**), amounting to an average of $+18.3$ kcal · mol^{-1} for the *endo*-series and only $+1.3$ kcal · mol^{-1} for the *exo*-series, again in excellent agreement with the experimental results in that we found *endo*-**3** but not *exo*-**3** in the reaction mixtures. It seems that the latter compounds are completely transformed into *exo*-**4**. Moreover, the pentacyclic *exo*-**4**, with the exception of *exo*-**4c**, are not disposed to undergo the rearrangement into *exo*-**5** by heterolytic cleavage of the C(8)–C(13) bond. The $\Delta\Delta H_f^\circ$ (**5** – **4**) values of the *exo*-series are indeed at an average of 14 kcal · mol^{-1} smaller than of the *endo*-series. One can, therefore, expect that the $\Delta H_f^{\neq}$ values for the final rearrangement step are larger in the *exo*-series than in the *endo*-series, particularly because the Me group at the three-membered ring is oriented towards the C(α)-atom of the substituents at C(10) (*cf. Fig. 1*; the calculated average interatomic C,C distance amounts to 385 pm and 394 pm according to the X-ray crystal structure of **4a**). The cleavage of the C(8)–C(13) bond moves the Me group at C(8) against the substituent at C(10) in the *exo*-series. This is, however, not the case in the *endo*-series, where the calculated average distance is almost the same (384 pm) and will not change very much for structural reasons during the cleavage process of the C(8)–C(13) bond[3]). When there is no substituent at C(10), as it follows from the thermal reaction of guaiazulene (**1c**) and ADM, the steric constraints seem to be smaller that finally *endo*-**4c** as well as *exo*-**4c** undergo the thermal rearrangement into *endo*-**5c** and *exo*-**5c**, respectively.

2.2. *Structure and Formation of* trans-**6**, **7**, *and* **9**. The first two product types (*i.e.*, **6** and **7**) were found in all reaction mixtures in amounts of 0.3–4%, whereas **9** was present in detectable amounts (0.2–1%) only in reaction mixtures containing **1a**. X-Ray crystal-structure analyses of *trans*-**6a** and **7a** (*Figs. 4* and *5*) revealed their amazing

[3]) The distances in the final *endo*- and *exo*-products are as follows: for **5a**: 388 and 356 pm, for **5b**: 346 and 321 pm, and for **5c**: 344 (X-ray: 347 pm) and 318 pm, respectively.

Table 2. *AM1-Calculated* ΔH_f° *Values of Products of Types* **3**, **4**, *and* **5** [a])

Enthalpy of formation [kcal·mol^{-1}]	*endo*-Series											
	3a	**4a**	**5a**	**3b**	**4b**	**5b**	**3c**	**4c**	**5c**	**3d**	**4d**	**5d**
ΔH_f°	−213.1	−195.5	−248.2	−203.8	−185.3	−243.4	−207.2	−188.4	−246.9	−169.9	−151.5	−208.6
$\Delta\Delta H_f^\circ$ [b])		+17.6	−52.7		+18.5	−58.1		+18.6	−58.5		+18.4	−57.1
	exo-Series											
	3a	**4a**	**5a**	**3b**	**4b**	**5b**	**3c**	**4c**	**5c**	**3d**	**4d**	**5d**
ΔH_f°	−208.5	−208.0	−245.0	−198.8	−197.6	−241.2	−201.9	−199.9	−245.9	−164.7	−163.4	−207.1
$\Delta\Delta H_f^\circ$ [b])		+0.5	−37.0		+2.2	−43.6		+1.0	−46.0		+1.3	−44.7

[a]) Calculated values for the conformationally most-relaxed structures with s-*trans*-oriented MeOCO groups. [b]) (ΔH_f° (**4**) − ΔH_f° (**3**)) and (ΔH_f° (**5**) − ΔH_f° (**4**)), respectively.

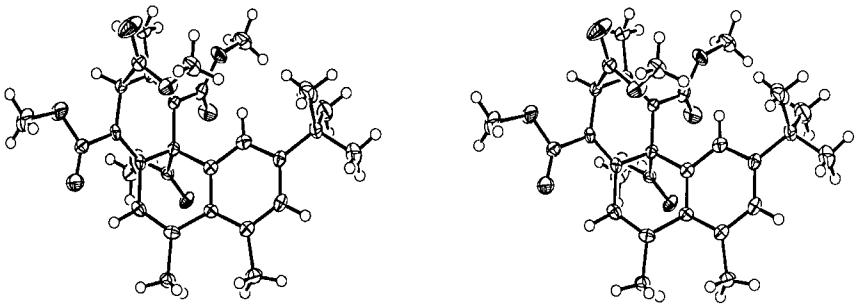

Fig. 4. *Stereoscopic view of the X-ray crystal structure of tetramethyl* trans-*6-(*tert-*butyl)-2,4a-dihydro-3,8,9-trimethylphenanthrene-1,2,4,4a-tetracarboxylate* (*trans*-**6a**)

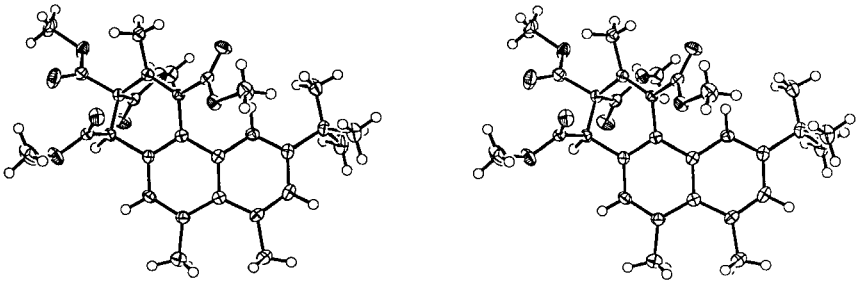

Fig. 5. *Stereoscopic view of the X-ray crystal structure of tetramethyl 6-(*tert-*butyl)-1,2-dihydro-3,8,9-trimethyl-[1-*^{2}*H]phenanthrene-1,2,2,4-tetracarboxylate* ([1-^{2}H]-**7a**)

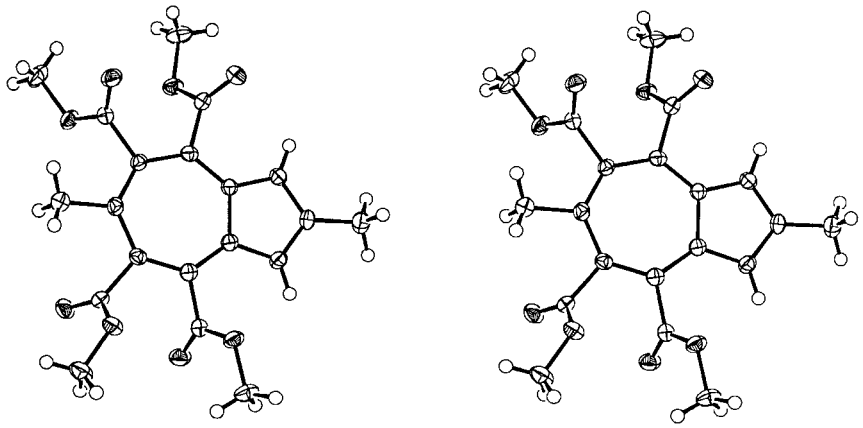

Fig. 6. *Stereoscopic view of the X-ray crystal structure of tetramethyl 2,6-dimethyl[1-^{2}H]azulene-4,5,7,8-tetracarboxylate* ([1-^{2}H]-**9**)

structures with Me–C(3) geometrically far away from the naphthalene core, which must arise from the original azulene skeleton of **1** in the presence of ADM. Most perplexing was the structure of **9**, anticipated by its pale blue color in solution with the longest-wavelength absorption at 585 nm (log ε 3.27) in MeCN and the simplicity of the NMR spectra. However, for certainty, we relied again on X-ray crystal-structure analysis (*cf. Fig. 6*).

Heating experiments with *trans*-**6a** and *trans*-**6b** demonstrated that *trans*-**6** is the primarily formed product that rearranges quantitatively into **7**. Since the structure of *trans*-**6a** and *trans*-**6b** could not be solved by NMR spectroscopy alone, we performed thermal experiments with *trans*-**6b** in MeOH in the presence of catalytic amounts of MeONa and found three products in the reaction mixture (*Scheme 7*), namely **7b**, which is also formed in the absence of base, and both, the tricarboxylates *trans*-**18b** and **19b** with one MeOCO group less than the starting material. The structures of *trans*-**18b** and **19b** were unequivocally determined by their spectroscopic data, in particular NMR. We assumed that either the angular MeOCO group of *trans*-**6b** or one of the MeOCO groups at C(2) of **7b** is split off as dimethyl carbonate after attack by MeO^-. Protonation of the formed dihydrophenanthrene anions by MeOH would then yield *trans*-**18b**, possibly accompanied by tautomerization. Oxidation by air would finally lead to the phenanthrene-1,2,4-tricarboxylate **19b**[4]). Control experiments with pure **7b**

[4]) The thermal formation of **7b** from *trans*-**6b** under basic conditions raised the question whether this rearrangement occurs generally *via* base-catalyzed loss of dimethyl carbonate that could recarboxylate dihydrophenanthrene anions of type *II* to form **7b**. We tested this assumption by the thermal reaction of guaiazulene (**1c**) with ADM in the presence of a threefold molar amount of di([$^2H_3$]methyl) carbonate and isolated both *trans*-**6c** and **7c**. MS and ^{1}H-NMR analyses showed that neither *trans*-**6c** nor **7c** contained any [$^2H_3$]MeO group at all. On this basis, it can be concluded that the transformation **6** → **7** is indeed a purely thermal intramolecular rearrangement (see later).

Scheme 7

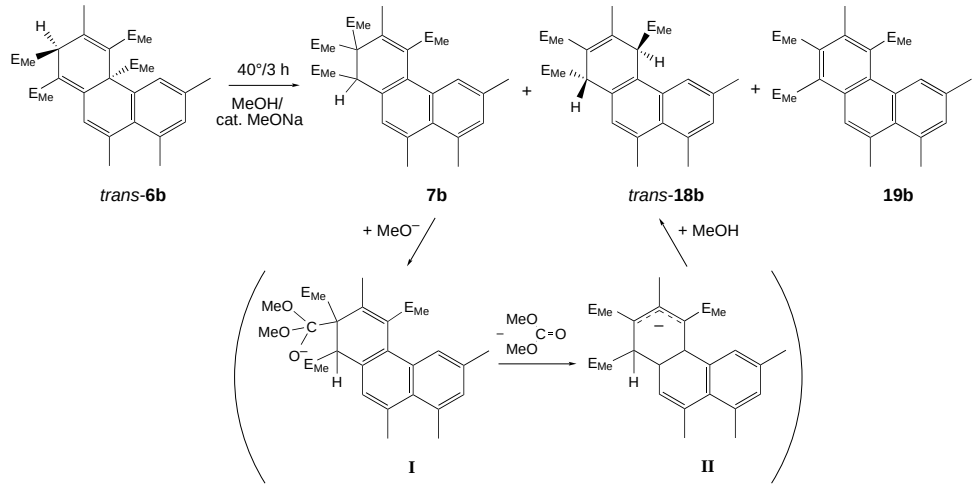

Scheme 8

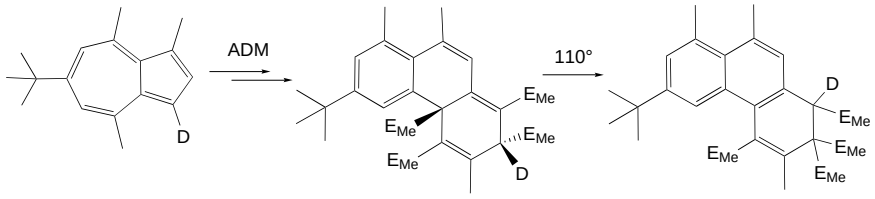

gave also *trans*-**18b** and **19b**, so that there is little doubt that solely **7b** is the precursor of the tricarboxylates.

Further interesting results came from the thermal transformation of [3-^{2}H]-**1a** and ADM (*vide supra*). Isolated and purified *trans*-**6a** (0.6%) carried the ^{2}H-label exclusively at C(2) and its thermal follow-up product **7** accordingly at C(1) (*Scheme 8*).

On the basis of these observations, we can only speculate on the thermal formation of *trans*-**6** from **1** and ADM in MeCN. An inspection of the structure of the central intermediate **14** (*Scheme 9*) leads to the congruous idea that it can only be the fragment Me–C(8a) that is later found as Me–C(3) in the final product *trans*-**6**, accompanied by a migration of the H-atom at C(2a), which is being bound at C(2) as shown by the labeling experiment. We have every reason to believe that the necessary skeletal transformations of **14** follow known reactivity patterns. Since the gross transformation requires a C_1-contraction of the seven-membered ring, it seems reasonable to postulate a cycloheptatriene $\rightleftharpoons$ norcaradiene equilibrium between **14** and **20**[5]), which should lie

[5]) See also the transformation of 4,5,6,7,8-pentamethylcyclohepta[*b*]furan-2(2*H*)-one into a (pentamethylphenyl)ethenyl fragment in the course of thermal cycloaddition reactions [16].

Scheme 9

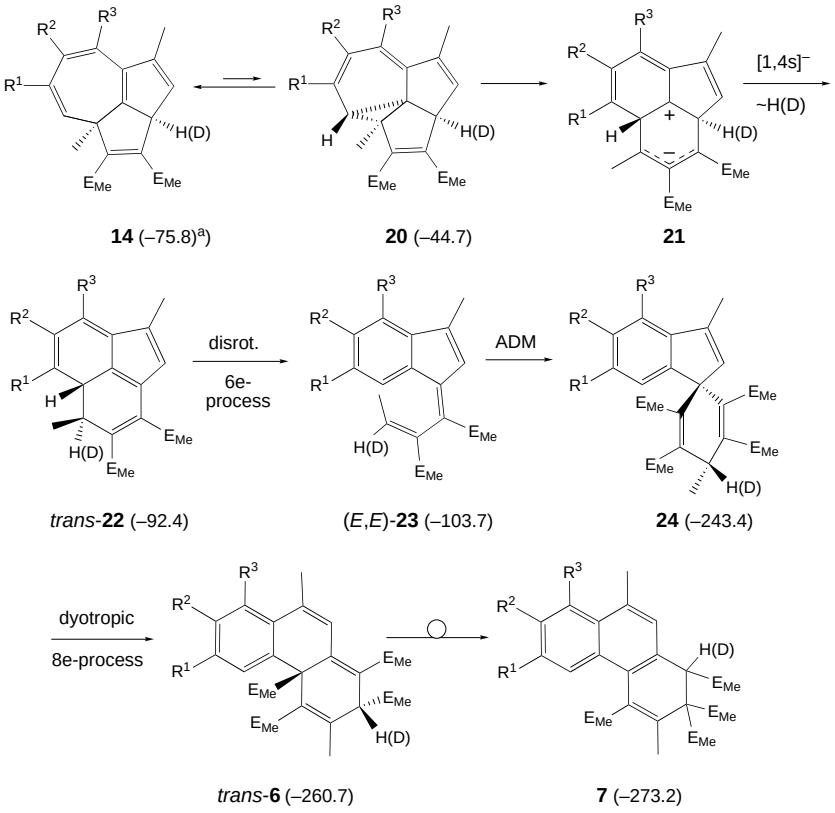

a) AM1-Calculated ΔH_f° values for the **b**-series (*cf. Scheme 1*) are given in parentheses. All values refer to the conformationally most-relaxed structures, whereby only s-*trans*-oriented MeOCO groups were taken into account.

far on the side of **14** according to AM1 calculations of ΔH_f° of the compounds of the **b**-series (*Scheme 9*). However, the accumulated structural strain will be substantially relieved by heterolytic cleavage of the original C(8a)–C(8b) bond. The zwitterions **21** formed should profit from charge stabilization by allylic resonance and extended cross-conjugation. A thermally allowed [1,4s]-H shift in the anionic part of **21** will give the neutral structure *trans*-**22**, which lies energetically by $> 45\ \text{kcal}\cdot\text{mol}^{-1}$ below the strained intermediate **20** and still by *ca.* $17\ \text{kcal}\cdot\text{mol}^{-1}$ below the starting tricyclic intermediate **14**. Intermediate *trans*-**22** contains a cyclohexa-1,3-diene substructure, well-suited for a thermally allowed disrotatory ring opening to give (*E*,*E*)-**23**, because the resulting structure represents an aromatic indene derivative substituted at C(1) with a but-2-enylidene residue. It is of importance to recognize that the disrotatory ring opening of *trans*-**22** can take place on structural grounds only by a single mode, which moves the two *trans*-oriented C(sp^3)-substituents (H and Me) inward, leading, therefore, specifically to the formation of (*E*,*E*)-**23** with the Me group at the side

Scheme 10

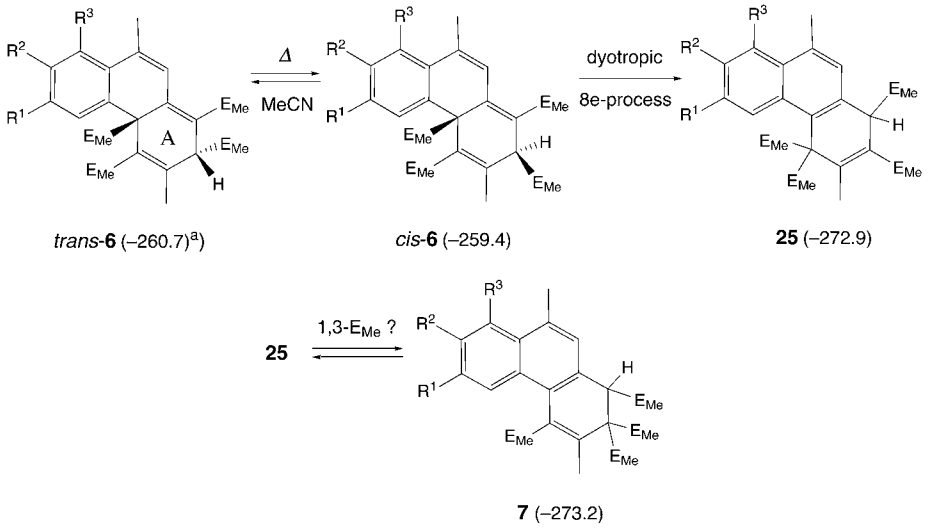

a) See *Scheme 9*.

chain formed pointing towards the aromatic ring. Intermediate (*E*,*E*)-**23** is fitted with an external diene system that is perfectly arranged for a [4+2] cycloaddition with ADM. The configuration at the C(2′)=C(3′) bond will be preserved hereby, so that the terminal Me group remains in a *syn*-relationship with the aromatic ring in the spiro-linked, C_s-symmetrical structure of **24**. We understand the next step to be one of the rare examples of a noncatalyzed, concerted, antarafacial dyotropic 8e-process, which results in the concomitant [1,2] migrations of the aromatic ring and the H-atom of **24** that originally belonged to C(2a) of **14**, thereby leading by C_1-expansion of the five-membered ring directly and specifically to *trans*-**6**[6]).

How the energetically favorable and noncatalyzed thermal rearrangement *trans*-**6**→**7** takes place is not clear at all at the moment (*cf. Scheme 9*). Other dihydrophenanthrene-tetracarboxylates, ring-A isomeric with **7**, seem not to be involved, since they all have similar AM1-calculated ΔH_f° values, indicating that mixtures of thermally equilibrated dihydrophenanthrene-tetracarboxylates together with **7** would have to be expected. An example of such an anticipated transformation is given in *Scheme 10*. Most questionable is the thermal 1,3-MeOCO migration that has to be postulated.

6) We refer here to the initial definition of *Reetz*, who named the above example 'type II' dyotropic reaction [17]. Most of the examples that had been reported so far represent 'type I' rearrangements [18], which consist of [1,2]-exchange shifts of functional groups (*cf.* [19] and refs. cit. therein) that may also occur under catalytic conditions (MgX_2 (X = Cl, Br) or BF_3; *cf.* [20] and refs. cit. therein). A number of intramolecular transhydrogenation reactions, which had been first analyzed and classified by *Woodward* and *Hoffmann* as group-transfer reactions [21], have been called more recently also 'dyotropic reactions' (*cf.* [22] and refs. cit. therein).

An initial homosigmatropic [1,5]-H shift in *trans*-**6** seems to be more appropriate to induce the transformation into **7** (*Scheme 11*). The intermediate cyclopropane derivative **26** lies energetically by only *ca.* 19 kcal · mol^{-1} above the starting material. The second step leading directly to **7** would represent a homosigmatropic [1,5]-MeOCO shift that would be, to the best of our knowledge, unprecedented. On the other hand, thermal sigmatropic [1,5]-acyl shifts in cyclohexa-1,3-dienes are well-known (*cf.* [23]). Nevertheless, the mechanism of the noncatalyzed formation of **7** from *trans*-**6** is still an open question.

Scheme 11

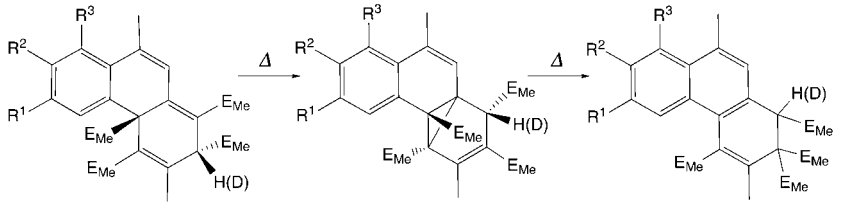

trans-**6** (–260.7)[a]) **26** (–242.1) **7** (–273.2)

[a]) See *Scheme 9*.

It remains to speculate on the formation of the azulene-4,5,7,8-tetracarboxylate **9** from **1a** and ADM, which might also be present in trace amounts in the reaction mixtures of the other azulenes. We believe that the structure of **9** supports the proposed mechanism for the formation of *trans*-**6** from the azulenes **1** and ADM, because a certain structural relationship between the spiro-linked intermediates **24** and **9** is obvious. The central question is, therefore, how the already correctly substituted spiro-linked six-membered ring of **24** can undergo ring-enlargement to the seven-membered ring of **9**, and how to get rid of parts of the aromatic ring with its substituents. In competition with a 8e-dyotropic reaction, the spiro-intermediate **24** may also undergo a reversible sigmatropic [1,5s]-C shift at its indene part, leading to the isoindene structure **27** (*Scheme 12*). Such types of sigmatropic reactions are well-known from indene/indene rearrangements which take place *via* corresponding energetically higher-lying isoindenes (*cf.* [23] and refs. cit. therein). The $\Delta\Delta H_f^\circ$ (**27** – **24**) values amount to 22 kcal · mol^{-1} in the present case[7]). A prototropic shift at **27**, attributable to the expected relatively high acidity of the H-atom at the tertiary C-atom, will yield the energetically relaxed tautomer *cis*-**28**. The latter is ideally disposed for an *anti*-addition of ADM to its cyclohexa-1,3-diene substructure[8]). The tetracyclic intermediate **29** thus formed has the right structural set-up for a retro-*Diels-Alder* reaction, which would lead to the formation of the azulene-tetracarboxylate **9** and the corresponding dimethyl phthalate **30**. We found no way to prove the presence of the latter in the reaction mixtures. However, we succeeded in isolation of **9** from the reaction mixture of [3-^{2}H]-

[7]) The ΔH_f° values in *Scheme 12* are given for the **b**-series of structures. The calculated $\Delta\Delta H_f^\circ$ values are almost the same for the structures of the **a**- and **b**-compounds and related types.

[8]) Of course, ADM may already be added to the cyclohexa-1,3-diene system of **27**, followed by a prototropic shift in the formed cycloadduct, resulting in the formation of **29**. Nevertheless, the intermediate gain in enthalpy is larger, as shown in *Scheme 12*, than the AM1 calculations suggest.

Scheme 12

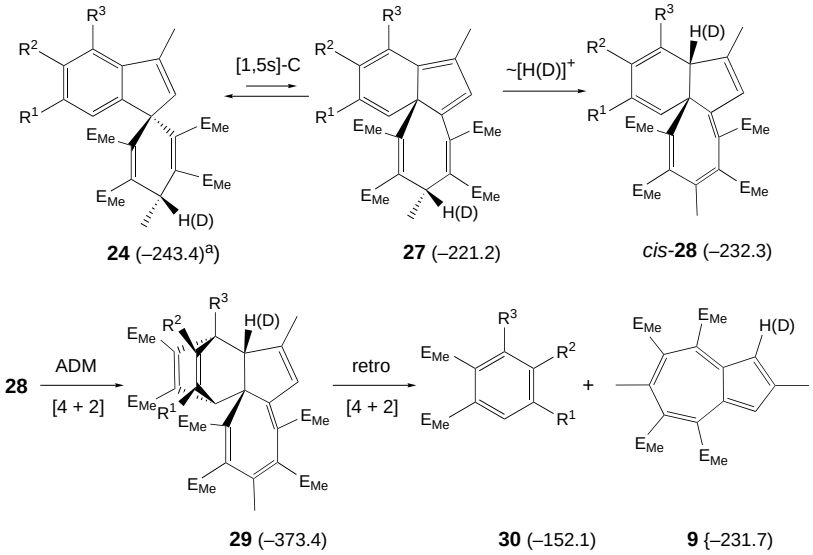

a) See *Scheme 9*.

1a and ADM. It contained, according to its ^{1}H-NMR and mass spectra, in total, one ^{2}H-atom at C(1/3), in agreement with the proposed mechanism of its formation (*Scheme 12*)[9]).

2.3. *Structure and Formation of* syn-**8**. We identified this product type in the reaction mixtures of **1a**, [3-^{2}H]-**1a**, and **1c**, and ADM in amounts of 0.5–3%. Crystals of *syn*-[11-^{2}H]-**8a** were suitable for an X-ray crystal-structure analysis, revealing the structure of a (1 + 2)-adduct (*Fig. 7*). Its skeleton was well-known to us, because compounds of this type were the main products in the *Lewis* acid catalyzed reaction of *peri*-methylated azulenes and ADM. An example is shown in *Scheme 13* [24]. Under neutral conditions and in the case in which C(8a) carries a H-atom, intermediates of type **14** may also react with ADM on their *exo*-site in a bisvinylogous ene reaction (*cf.* [6]) or, in the presence of an acid, may undergo a prototropic shift to yield the corresponding *cis*-2a,8b-dihydro-3,4-ethenoazulenes [11][24]. The [4 + 2] cycloaddition of **14** and ADM can take place principally on the *endo*-**14** or *exo*-face of **14**, whereby the syn-adducts possess slightly smaller ΔH_f° values than the *anti*-adducts resulting from the *exo*-path. The AM1-calculated difference between the two unsaturated tetracyclic basal skeletons is -6.8 kcal · mol^{-1} in favor of the *anti*-arrangement and is reduced to -3.5 kcal · mol^{-1} in the case of *syn*-**8a** *vs. anti*-**8a**. Since, in all reactions so far investigated [24], only the *syn*-arranged products of type **8** or **31** and **32** are formed speaks for a steric hindrance of the concerted *exo*-approach of ADM to C(3) and C(8b) by the two substituents at C(2a) and C(8a) in reactants of type **14**. It is of interest to note that the

9) The ^{2}H-content of **9** should be in principle the same as that of [3-^{2}H]-**1a**, *i.e.*, in total, 0.5 ^{2}H at the two equivalent positions C(1,3). It seems, therefore, that primary kinetic H/^{2}H isotope effects, which will be in favor of an increase in the ^{2}H-content, are involved in the reaction (see also *Exper. Part*).

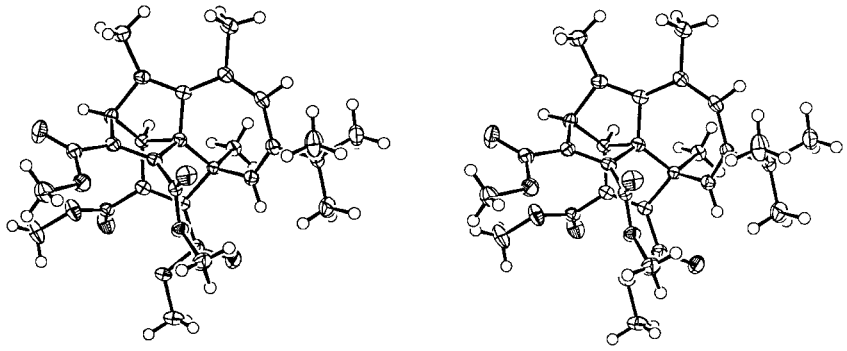

Fig. 7. *Stereoscopic view of the X-ray crystal structure of tetramethyl* syn-*6-(*tert-*butyl)-2,4,8-trimetyl[11-*^{2}*H]tetracyclo[6.3.3.0*^{3,12}*.0*$^{11,1\,2}$*]tetradeca-2,4,6,9,13-pentaene-9,10,13,14-tetracarboxylate* (*syn*-[11-^{2}H]-**8a**)

ΔH_f° value of *syn*-**8a** lies with -197.3 kcal·mol^{-1} by >11 kcal·mol^{-1} above those of the [4 + 2] adducts *endo*-**3a** and *exo*-**3a** of **17a** (*cf. Scheme 5* and *Table 2*), whereas the ΔH_f° values of **14a** (-85.1 kcal·mol^{-1}) and **17a** (-85.6 kcal·mol^{-}) are close together. This means that the activation energy (*E*a) of the cycloaddition reaction of ADM with the central intermediates **14** must in general be distinctly smaller than with their [1,5]-H-shifted forms **17**.

The compounds of type *syn*-**8** (or *syn*-**31**/**32**) are characterized by two specific structural features, namely a 'frozen' sickle-like conformation of a triene system with torsion angles, which still allow a high degree of conjugation together with a key norbornadiene segment with well-defined dihedral angles around C(1) and

Scheme 13

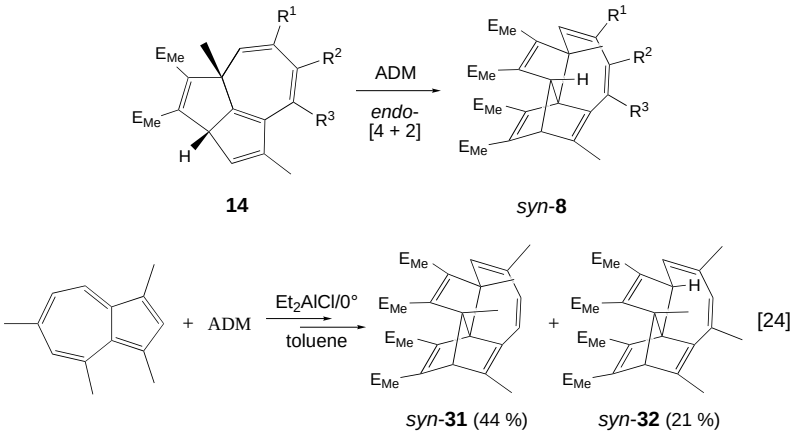

C(11)[10]). As a consequence, both *syn*-**8a** and *syn*-**8c** as well as the other compounds of this type exhibit in their UV/VIS spectra (MeCN) a strong $\pi \rightarrow \pi^*$ transition at 290 nm (log ε 3.85 and 3.74, respectively) and a second one, as a shoulder, at 343 and 344 nm (log ε 3.33 and 3.40, respectively)[11]) as well as a comparably small J_{vic} value of 1.5 Hz between H–C(1) and H–C(11) as typical for all bicyclo[2.2.1]heptadienes (*cf.* [25]).

2.4. *Characterization of the Heptalene-4,5-dicarboxylates* **2**. As mentioned in the *Introduction* we were mainly interested in investigating the influence of conjugated substituents (Ph, 3,5-$Me_2C_6H_3$, and 1,1′-biphenyl-4-yl) at C(8) on the UV/VIS spectra of **2** in comparison with those of their DBS isomers, the heptalene-1,2-dicarboxylates, **2′**. The latter were exclusively prepared in analytical amounts on heating or irradiation of **2** (*cf.* [26]) and, therefore, solely characterized by their UV/VIS spectra (see below).

We performed X-ray crystal-structure determinations of the 8-phenyl- and the 8-(1,1′-biphenyl-4-yl)-substituted dicarboxylates **2d** and **2f**, respectively, and also for **2a**, for which an older X-ray crystal-structure analysis together with that of its DBS form **2′a** already exists [26]. A stereoscopic view of the crystal structure of **2f** is displayed in *Fig. 8*, and some relevant data of all three heptalenes are listed in *Table 3*. The differences in the structural parameters of all three heptalenes are as expected marginal and mostly within the standard deviations of the measurements. The torsion angles, defined mainly by the spatial shape and the conjugation within the two seven-membered rings of the heptalenes, are close together, especially those of the MeOCO-substituted ring, in full agreement with the observed ^3J(H–C(2),H–C(3)) = 5.9 Hz for all 4 heptalenes with occupied *peri*-positions. The bond angle at C(8) of **2d** and **2f** with the π-substituents is slightly enlarged in comparison with **2a** with σ-substitution at C(8). The expected conjugation of the π-substituents with the core C=C bonds is also indicated by the observed small cisoid Θ(C(9)–C(8)–C(1′)–C(2″)) values. The angle between the planes of the two phenyl rings in **2f** is 44.4(1)°.

The UV/VIS spectra of **2a** and **2d**–**2f** and their corresponding DBS forms **2′**, as measured with the photo-diode-array detector of an HPLC system are displayed in *Figs. 9–12* (for details and definitions, see [7]). The reference spectra of **2a** and **2′a** (*Fig. 9*) are, as expected, very similar to those of **2b** and **2′b** [7]. Heptalene band *I* of **2′a** appears as a weak broad absorption at *ca.* 390 nm, well-separated from the shoulder of heptalene band *II* at 315 nm and followed by the strong absorption of heptalene band *III* at 270 nm. The DBS isomer **2a**, which carries Me–C(1) in conjugative interaction with MeOCO–C(4), shows heptalene band *I* as a broad shoulder, again at *ca*. 390 nm, however, with slightly enhanced intensity in comparison with **2′a**. Heptalene band *II* is just recognizable as a shoulder at *ca.* 320 nm, whereas heptalene band *III* appears at 265 nm with a faintly visible shoulder at its longer-wavelength flank. The habitus of the spectra of the π-substituted heptalenes **2** and **2′** is, as expected, largely consonant and do not deviate much from that of **2a** and **2′a**, respectively. Nevertheless, there are small

---

[10]) The torsion angles of the triene system in the X-ray crystal-structure of *syn*-[11-^{2}H]-**8a** amount to 20.3(3)° (at C(5)–C(6)) and 161.9(2)° (at C(3)–C(4)), whereas the AM1-calculated structure gives as a result torsion angles of 35.4° and 165.0°, respectively. The torsion angle of H–C(1)–C(11)–H at the norbornadiene substructure amounts to 64.6° (X-ray) and 61.2° (AM1), close to that of the parent structure (63.4°).

[11]) The λ_{max} values of the two model compounds in MeCN are as follows; *syn*-**31**: 280 (sh, 3.71) and 348 (sh, 3.17); *syn*-**32**: 289 (3.77) and 335 (sh, 3.38) [24].

Table 3. *Skeletal Parameters from the X-Ray Crystal-Structures of the Heptalene-4,5-dicarboxylates* **2a**, **2d**, *and* **2f** [a])

Parameter[b])	**2a**	**2d**	**2f**
Interatomic distances *d* [pm]			
C(1)–C(2)	133.7(2)	134.4(2)	133.8(3)
C(6)–C(7)	133.9(2)	134.2(2)	133.6(3)
C(8)–C(9)	134.9(2)	135.9(2)	135.8(3)
C(10)–C(10a)	134.3(2)	135.4(2)	135.3(3)
Bond angles ϑ [°]			
C(2)–C(3)-C(4)	127.5(1)	127.2(1)	127.3(2)
C(7)–C(8)–C(9)	122.4(1)	123.2(1)	123.2(2)
cisoid Torsion angles Θ [°]			
C(1)–C(2)–C(3)–C(4)	32.5(2)	30.0(3)	29.9(4)
C(3)–C(4)–C(5)–C(5a)	– 31.5(2)	– 31.6(3)	– 32.7(4)
C(6)–C(7)–C(8)–C(9)	35.0(2)	35.8(3)	35.9(4)
C(8)–C(9)–C(10)–C(10a)	– 34.4(2)	– 33.7(3)	– 36.0(4)
C(1)–C(10a)–C(5a)–C(5)	63.9(2);	62.5(2)	65.8(3)
C(6)–C(5a)–C(10a)–C(10)	65.7(2)	64.8(2)	66.0(3)
transoid Torsion angles Θ [°]			
C(5)–C(5a)–C(6)–C(7)	122.3(2)	120.4(2)	124.0(3)
C(2)–C(1)–C(10a)–C(10)	119.2(2)	121.7(2)	124.1(3)
C(5)–C(5a)–C(10a)–C(10)	– 118.7(2)	– 119.2(2)	– 120.0(3)
C(1)–C(10a)–C(5a)–C(6)	– 111.7(1)	– 113.5(1)	– 108.1(3)
Lateral torsion angles Θ [°]			
C(10)–C(9)–C(8)–C(1′)	– 173.5(1)	– 178.1(1)	– 172.2(2)
C(9)–C(8)–C(1′)–C(2′)	–	33.2(2)	23.6(4)
C(3)–C(4)–C=O	165.4(1)	– 19.9(2)	– 155.7(2)
C(5a)–C(5)–C=O	– 46.6(2)	– 48.4(2)	140.3(2)

[a]) Data collection at 160(1) (**2a**) and 173(1)K (**2d** and **2f**), respectively; for an older crystal-structure analysis of **2a** at 170 K, see [26]. [b]) Standard uncertainties in parentheses.

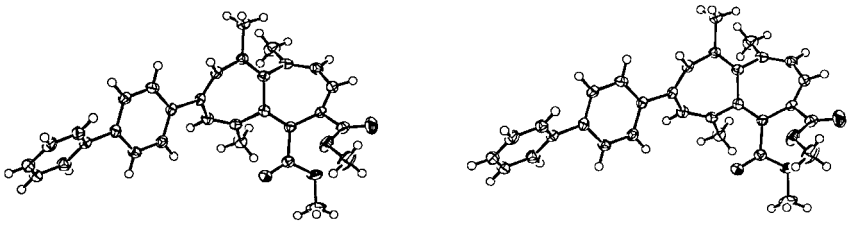

Fig. 8. *Stereoscopic view of the X-ray crystal structure of dimethyl 8-(1,1′-biphenyl-4-yl)-1,6,10-trimethylheptalene-4,5-dicarboxylate* (**2f**)

differences. Whereas the broad heptalene band *I* appears in all spectra at almost the same wavelength with the weakest intensity, the heptalene band *II* with respect to **2a** and **2′a** is bathochromically shifted by *ca.* 10–15 nm and enhanced in its intensity. It represents in the spectra of the Ph-substituted heptalenes **2d** and **2e** a well-formed shoulder, which is much less distinguished in the spectrum of the 4-(1,1′-biphenyl-4-yl)-

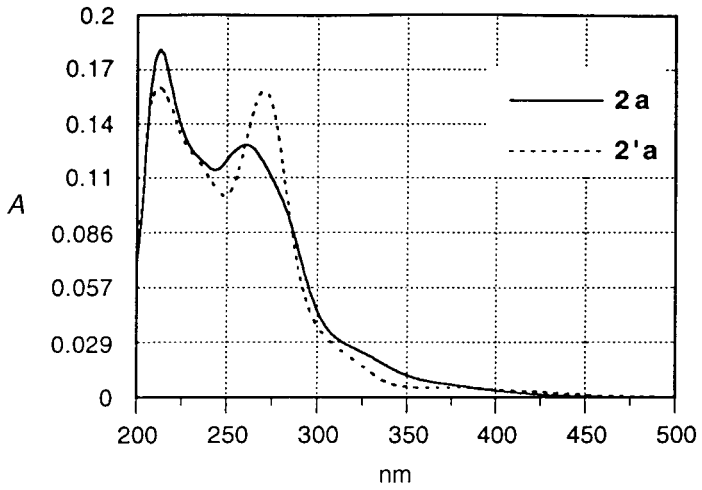

Fig. 9. *UV/VIS Spectrum of dimethyl 8-*(tert-*butyl)-1,6,10-trimethylheptalene-4,5-dicarboxylate* (**2a**) *and its DBS isomer dimethyl 8-*(tert-*butyl)-5,6,10-trimethylheptalene-1,2-dicarboxylate* (**2′a**)

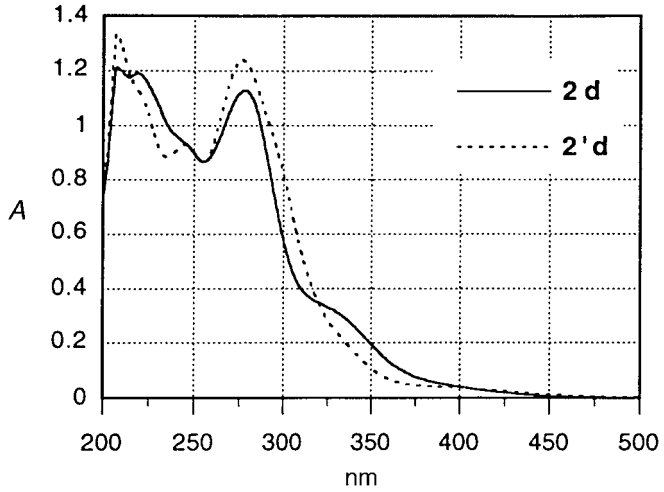

Fig. 10. *UV/VIS Spectrum of dimethyl 1,6,10-trimethyl-8-phenylheptalene-4,5-dicarboxylate* (**2d**) *and its DBS isomer dimethyl 5,6,10-trimethyl-8-phenylheptalene-1,2-dicarboxylate* (**2′d**)

substituted heptalene **2f**. This band is nearly not recognizable in the spectra of the corresponding DBS isomers **2′d**–**2′f**, and its position can only be estimated to be in the range of 335–345 nm (*cf. Table 4*). Clear distinctions can be seen in the heptalene band *III* of **2′d**–**2′f**, which is bathochromically shifted by at least 12 nm with respect to **2′a**. In going from **2′a** *via* **2′d** and **2′e** to **2′f**, one observes a splitting of this band into two (see also *Table 4*). This absorption band is almost symmetric in the case of **2′a**, but becomes slightly asymmetric for **2′d** in form of a faint shoulder at the longer-wavelength flank of this band. The hint of a shoulder becomes, in the case of **2′e**, a well-recognizable

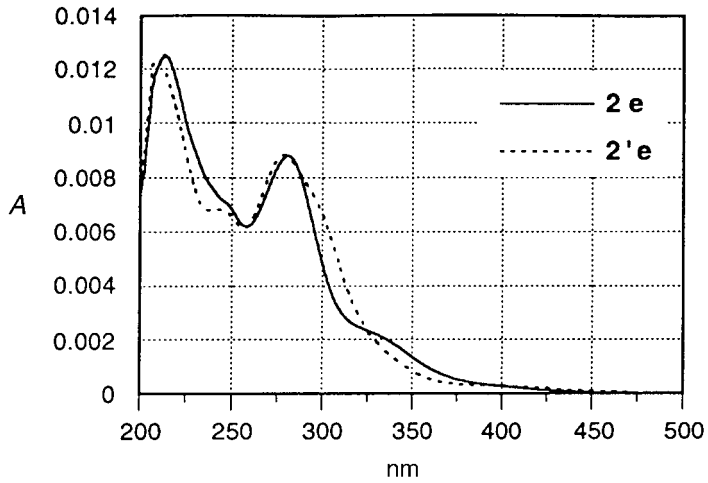

Fig. 11. *UV/VIS Spectrum of dimethyl 8-(3,5-dimethylphenyl)-1,6,10-trimethylheptalene-4,5-dicarboxylate* (**2e**) *and its DBS isomer dimethyl 8-(3,5-dimethylphenyl)-5,6,10-trimethylheptalene-1,2-dicarboxylate* (**2′e**)

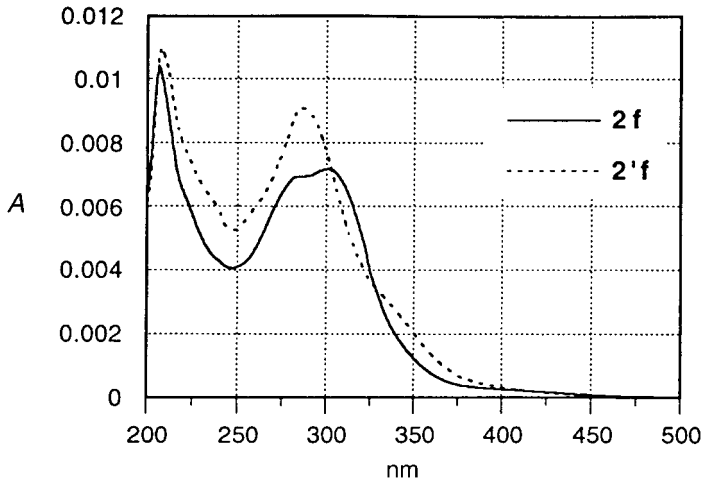

Fig. 12. *UV/VIS Spectrum of dimethyl 8-(4-biphenyl)-1,6,10-trimethylheptalene-4,5-dicarboxylate* (**2f**) *and its DBS isomer dimethyl 8-(4-biphenyl)-5,6,10-trimethylheptalene-1,2-dicarboxylate* (**2′f**)

shoulder at *ca.* 297 nm, which develops to a second longer-wavelength maximum at 302 nm for the 4-(1,1′-biphenyl-4-yl)-substituted heptalene **2′f**. The heptalene band *III* remains more or less symmetric for the series of the heptalene-4,5-dicarboxylates **2**, whereby the π-substituents at C(8) cause a slight displacement by *ca.* 8–15 nm to longer wavelength (see also *Table 4*).

It can be concluded from this structural and spectral study that π-substituents at C(8) of heptalenes will not alter their general shape, but may well differentiate the electronic absorption behavior of the heptalenes and their DBS isomers in a way that

Table 4. *UV/VIS Spectral Data of the Heptalene-4,5-dicarboxylates* **2** *and Their DBS Forms* **2′**[a])

Heptalene-dicarboxylate[c])	Heptalene Bands[b])		
	I	II	III
2a	*ca.* 390 (sh, 0.03)	*ca.* 322 (sh, 0.18)	261 (1.00)
2′a	*ca.* 390 (0.03)	*ca.* 316 (sh, 0.14)	271 (1.00)
2d	*ca.* 390 (sh, 0.04)	*ca.* 325 (sh, 0.29)	278 (1.00)
2′d	*ca.* 390 (0.03)	*ca.* 330 (sh, 0.20)	277 (1.00)
2e	*ca.* 390 (sh, 0.04)	*ca.* 330 (sh, 0.27)	278 (1.00)
2′e	*ca.* 390 (0.04)	*ca.* 335 (sh, 0.21)	297 (sh, 0.83) 278 (1.00)
2f	*ca.* 390 (sh, 0.04)	*ca.* 335 (sh, 0.35)	288 (1.00)
2′f	*ca.* 390 (sh, 0.04)	*ca.* 345 (sh, 0.20)	302 (1.00) 283 (0.97)

[a]) Spectra recorded in hexane/*i*-PrOH 95 : 5 during HPLC separation of **2** and **2′**. [b]) λ_{max} in nm; rel. intensities in parentheses. [c]) See *Scheme 1* for substituents.

double-wavelength photochemical switching between these forms will be possible and effective.

We thank our NMR laboratory, in particular *Nadja Walch*, *Martin Binder*, and Dr. *Gudrun Hopp* for specific NMR measurements, Prof. *M. Hesse* and his group for mass-spectrometric measurements, and, finally, *Peter Uebelhart* for the help with *Figs. 9–12*. The financial support of this work by the *Swiss National Science Foundation* is gratefully acknowledged.

Experimental Part

General. See [27]. ^{2}H-NMR spectra at 92 MHz were measured on a *Bruker DRX-600* spectrometer. Anal. HPLC on a *Waters* instrument with a column (12.5 cm × 4 mm) of *Spherisorb* (3 μm); eluant: hexane/i-PrOH 95 : 5. Crystallizations and recrystallizations were performed in Et_2O/hexane mixtures, if not otherwise stated.

1. Azulenes. – *General*. Guaiazulene (= 7-isopropyl-1,4-dimethylazulene; **1c**) was available from *Fluka*. We synthesized the other azulenes on *Hafner*'s route from 2,6-dimethyl-4-pyrone (*Fluka*) *via* the corresponding pyrylium tetrafluoroborates [10] (see also [26][28]). The thus formed 6-R-4,6-dimethylazulenes were then formylated and reduced with $NaBH_4$ in CF_3COOH/CH_2Cl_2 [29] (see also [8][30]).

1.1. *6-(*tert*-Butyl)-1,4,8-trimethyl[3-^{2}H]azulene* ([3-^{2}H]-**1a**). Nonlabeled **1a** (0.452 g, 2.00 mmol) [26] was dissolved in MeO[^{2}H] (3.6 ml), and two drops of AcO[^{2}H] (*ca.* 0.02 g) were added. The mixture was heated during 6 h at 100° in an autoclave vessel under Ar. The solvent was removed by distillation and the residue subjected to CC on alumina (act. III) with hexane. ^{1}H-NMR (300 MHz, $CDCl_3$): 7.44 (*s*, H–C(2)); 7.21 (*s*, H–C(3)), residual amount of H according to H–C(2) or Me–C(1) as standard for integration: 48%; *i.e.*, ^{2}H = 52%.

1.2. *1,4,8-Trimethyl-6-phenylazulene* (**1d**). 1.2.1. *4,8-Dimethyl-6-phenylazulene*. Yield 46%. Blue crystals. M.p. 100–101°. R_f (hexane) 0.27. IR (KBr): 3072*w*, 2920*w*, 1569*s*, 1484*s*, 1368*m*, 1330*m*, 1261*w*, 1067*m*, 926*w*, 866*s*, 764*s*, 738*s*, 703*s*. ^{1}H-NMR (300 MHz, $CDCl_3$): 7.77 (*t*, ^3J = 3.8, H–C(2)); 7.65 (*dd*, J_0 = 6.8, J_m = 1.5, H–C(2′,6′)); 7.52–7.40 (*m*, 3 H of Ph); 7.45 (*d*, ^3J = 3.9, H–C(1,3)); 7.37 (*s*, H–C(5,7); 2.99 (*s*, Me–C(4,8)). ^{13}C-NMR (75 MHz, $CDCl_3$): 148.72 (*s*, C(1′)); 146.28 (*s*, C(3a,8a)); 145.66 (*s*, C(4,8)); 136.43 (*s*, C(6)); 133.75 (*d*, C(2)); 128.70 (*d*, C(5,7)); 128.56 (*d*, C(3′,5′)); 127.65 (*d*, C(4′)); 126.37 (*d*, C(2′,6′)); 116.45 (*d*, C(1,3)); 25.29 (*q*, *Me*–C(4,8)). EI-MS ($C_{18}H_{16}$; 232.33): 232.2 (100, $M^{+\cdot}$), 217.1 (13, $[M-Me]^+$), 216.2 ($[M-(Me+H)]^{+\cdot}$), 215.0 (31, $[M-(Me+2\,H]^{+\cdot}$), 202.0 (20), 188.9 (7), 164.9 (4).

1.2.2. *4,8-Dimethyl-6-phenylazulene-1-carbaldehyde*. Yield of *Vilsmeyer* formylation: 98%. Red crystals. M.p. 98–99°. R_f (hexane/Et_2O 1:1) 0.32. IR (KBr): 3448*m*, 3053*w*, 1628*s*, 1578*s*, 1540*m*, 1498w, 1446m, 1349s, 1216w, 1107m, 1090m, 914w, 791m, 769s, 700s. ^{1}H-NMR (300 MHz, $CDCl_3$): 10.71 (*s*, OHC–C(1)); 8.37 (*d*, ^3J = 4.5, H–C(2)); 7.69–7.62 (*m*, 3 H of Ph, H–C(7)); 7.55–7.46 (*m*, 2 H of Ph, H–C(5)); 7.40 (*d*, ^3J = 4.5, H–C(3)); 3.27 (*s*, Me–C(8)); 3.01 (*s*, Me–C(4)). ^{13}C-NMR (75 MHz, $CDCl_3$): 187.04 (*d*, OH*C*–C(1)); 149.97

(*s*, C(6)); 148.21 (*s*, C(8)); 148.08 (*s*, C(4)); 144.62 (*s*, C(1′)); 142.80 (*s*, C(3a)); 138.87 (*d*, C(2)); 137.17 (*s*, C(8a)); 132.47 (*d*, C(7)); 131.17 (*d*, C(5)); 130.57 (*s*, C(1)); 128.87 (*d*, C(2′,6′)); 128.64 (*d*, C(3′,5′)); 128.42 (*d*, C(4′)); 117.55 (*d*, C(3)); 31.13 (*q*, *Me*–C(8)); 26.40 (*q*, *Me*–C(4)). EI-MS ($C_{19}H_{16}O$; 260.34): 260.1 (22, $M^{+\bullet}$), 250.1 (33); 245.1 (14, $[M-Me]^+$), 243.1 ($[M-(Me+2\,H)]^{+\bullet}$), 207.1 (15), 185 (22), 173.1 (100).

1.2.3. *Azulene* **1d**. Yield of $NaBH_4$ reduction: 97%. Blue crystals. M.p. 102–103°. R_f (hexane) 0.25. IR (KBr): 3098*w*, 3065*w*, 2920*m*, 1570*s*, 1508*s*, 1491*s*, 1368*m*, 1299*m*, 1108*m*, 998*m*, 860*s*, 776*s*, 763*s*, 702*s*. ^{1}H-NMR (300 MHz, $CDCl_3$): 7.63 (*dd*, $J_0=6.9$, $J_m=1.5$, H–C(2′,6′)); 7.53 (*d*, $^3J=3.9$, H–C(2)); 7.48–7.39 (*m*, H–C(3′,4′,5′)); 7.33 (*d*, $^3J=3.9$, H–C(3)); 7.15 (*s*, H–C(5,7)); 3.10 (*s*, Me–C(8)); 2.91 (*s*, Me–C(1)); 2.90 (*s*, Me–C(4)). EI-MS ($C_{19}H_{18}$; 246.35): 246.2 (100, $M^{+\bullet}$), 231.1 (66, $[M-Me]^+$), 215 (51, $[M-(Me+CH_4)]^+$), 202 (20), 188.9 (11), 143.0 (14).

1.3. *6-(3,5-Dimethylphenyl)-1,4,8-trimethylazulene* (**1e**). 1.3.1. *6-(3,5-Dimethylphenyl)-4,8-dimethylazulene*. Yield 50%. Blue crystals. M.p. 124–125°. R_f (hexane) 0.24. IR (KBr): 3108*w*, 2910*m*, 1570*s*, 1483*s*, 1372*s*, 1276*m*, 1073*m*, 1009*m*, 845*s*, 754*s*, 607*m*. ^{1}H-NMR (300 MHz, $CDCl_3$): 7.75 (*t*, $^3J=3.9$, H–C(2)); 7.43 (*d*, $^3J=3.9$, H–C(1,3)); 7.35 (*s*, H–C(5,7)); 7.24 (*s*, H–C(2′,6′)); 7.07 (*s*, H–C(4′)); 2.98 (*s*, Me–C(4,8)); 2.43 (*s*, Me–C(3′,5′)). ^{13}C-NMR (75 MHz, $CDCl_3$): 149.10 (*s*, C(1′)); 146.31 (*s*, C(3a,8a)); 145.62 (*s*, C(4,8)); 138.13 (*s*, C(3′,5′)); 136.40 (*s*, C(6)); 133.52 (*d*, C(2)); 129.29 (*d*, C(4′)); 126.59 (*d*, C(2′,6′)); 126.37 (*d*, C(5,7)); 116.28 (*d*, C(1,3)); 25.28 (*q*, *Me*–C(4,8)); 21.37 (*q*, *Me*–C(3′,5′)). EI-MS: 260.1 (55, $M^{+\bullet}$), 235 (12), 220.0 (10, $[M-MeC{\equiv}CH]^{+\bullet}$), 173.0 (100). Anal. calc. for $C_{20}H_{20}$ (260.38): C 92.26, H 7.74; found: C 92.00, H 7.94.

1.3.2. *6-(3,5-Dimethylphenyl)-4,8-dimethylazulene-1-carbaldehyde*. Yield of *Vilsmeyer* formylation: 89%. Red crystals. M.p. 128–129°. R_f (hexane/Et_2O 1:1) 0.36. ^{1}H-NMR (300 MHz, $CDCl_3$): 10.71 (*s*, OHC–C(1)); 8.36 (*d*, $^3J=4.5$, H–C(2)); 7.68 (*s*, H–C(7)); 7.65 (*s*, H–C(5)); 7.39 (*d*, $^3J=4.5$, H–C(3)); 7.24 (*s*, H–C(2′,6′); 7.11 (*s*, H–C(4′)); 3.27 (*s*, Me–C(8)); 3.02 (*s*, Me–C(4)); 2.44 (*s*, Me–C(3′,5′)). ^{13}C-NMR (75 MHz, $CDCl_3$): 187.06 (*s*, OH*C*–C(1)); 150.38 (*s*, C(6)); 148.15 (*s*, C(8)); 148.01 (*s*, C(4)); 144.64 (*s*, C(1′)); 142.76 (*s*, C(3a)); 138.62 (*d*, C(2)); 138.52 (*s*, C(3′,5′)); 137.16 (*s*, C(8a)); 132.49 (*d*, C(7)); 131.18 (*d*, C(5)); 130.47 (*s*, C(1)); 130.05 (*d*, C(4′)); 126.52 (*d*, C(2′,6′)); 117.43 (*d*, C(3)); 31.14 (*q*, *Me*–C(8)); 26.39 (*q*, *Me*–C(4)); 21.34 (*q*, *Me*–C(3′,5′)).

1.3.3. *Azulene* **1e**. Yield of $NaBH_4$ reduction: 62%. Blue crystals. M.p. 125–126°. R_f (hexane) 0.21. ^{1}H-NMR (300 MHz, $CDCl_3$): 7.52 (*d*, $^3J=3.9$, H–C(2)); 7.33 (*d*, $^3J=3.9$, H–C(3)); 7.23 (*s*, H–C(2′,6′)); 7.14 (*s*, H–C(5,7)); 7.06 (*s*, H–C(4′)); 3.11 (*s*, Me–C(8)); 2.92 (*s*, Me–C(1)); 2.90 (*s*, Me–C(4)); 2.42 (*s*, Me–C(3′,5′)).

1.4. *6-(1,1′-Biphenyl-4-yl)-1,4,8-trimethylazulene* (**1f**). 1.4.1. *6-(1,1′-4-Biphenyl-4-yl)-4,8-dimethylazulene*. Yield 30%. Blue crystals. M.p. 167–168°. R_f (hexane/Et_2O 9:1) 0.58. IR (KBr): 3028*m*, 2920*m*, 1598*w*, 1538*m*, 1484*s*, 1446*m*, 1373*m*, 1216*m*, 1005*s*, 836*s*, 768*s*, 678*m*, 599*m*. ^{1}H-NMR (300 MHz, $CDCl_3$): 7.76 (*t*, $^3J=4.0$, H–C(2)); 7.72 (*s*, H–C(2′,3′,5′,6′)); 7.67 (*d*, $J_o=7.2$, H–C(2″,6″)); 7.51 (*t*, $J_o=7.5$, H–C(3″,5″)); 7.45 (*d*, $^3J=4.0$, H–C(1,3)); 7.41 (br. *s*, H–C(5,7)); 7.38 (*t*, $J_o=7.4$, H–C(4″)); 2.99 (*s*, Me–C(4,8)). ^{13}C-NMR (75 MHz, $CDCl_3$): 148.21 (*s*, C(1′)); 145.67 (*s*, C(4,8)); 145.13 (*s*, C(3a,8a)); 140.64 (*s*, C(6′)); 140.53 (*s*, C(1″)); 136.45 (*s*, C(6)); 133.79 (*s*, C(2)); 129.14 (*d*, C(3′,5′)); 128.86 (*d*, C(5,7)); 127.51 (*d*, C(4″)); 127.24 (*d*, C(3″,5″)); 127.11 (*d*, C(2″,6″)); 126.20 (*d*, C(2′,6′)); 116.52 (*d*, C(1,3)); 25.33 (*q*, *Me*–C(4,8)). EI-MS ($C_{24}H_{20}$; 308.42): 309.1 (16, $[M+1]^{+\bullet}$), 308.1 (100, $M^{+\bullet}$), 307.2 (11, $[M-1]^+$), 293.0 (4, $[M-Me]^+$), 292.0 (6, $[M-(Me+H]^{+\bullet}$), 291.0 (9, $[M-(Me+2\,H]^+$), 252 (5, $[M-(MeC{\equiv}CH+Me+H]^{+\bullet}$), 216.1 (7, $[M-(Ph+Me+H]^+$), 215.0 (20, $[M-(Ph+Me+2\,H]^{+\bullet}$), 154.2 (29, $[M-(Biph+H)]^{+\bullet}$), 152.1 (16, $[M-(Biph+3\,H)]^{+\bullet}$), 115.1 (15, $[Biph]^+$), 77.0 (23, $[Ph]^+$).

1.4.2. *6-(1,1′-Biphenyl-4-yl)-4,8-dimethylazulene-1-carbaldehyde*. Yield of *Vilsmeyer* formylation: 88%. Red crystals. M.p. 169–170°. R_f (hexane/Et_2O 1:1) 0.38. IR (KBr): 3028*w*, 1634*s*, 1575*w*, 1538*m*, 199*m*, 1486*s*, 1350*s*, 1214*m*, 1063*m*, 839*m*, 793*w*, 699*s*. ^{1}H-NMR (600 MHz, $CDCl_3$): 10.71 (*s*, OHC–C(1)); 8.38 (*d*, $^3J=4.5$, H–C(2)); 7.751, 7.725 (AA′BB′, $J_{AB}=8.5$, H–C(3′,5′), H–C(2′,6′)); 7.735 (br. *s*, H–C(7)); 7.712 (*s*, H–C(5)); 7.68 (*dd*, $J_o=8.1$, $J_m=1.2$, H–C(2″,6″)); 7.50 (*t*, $J_o=7.7$, H–C(3″,5″)); 7.40 (*d*, $^3J=4.4$, H–C(3)); 7.41 (*tt*, $J_o=7.4$, $J_m=1.2$, H–C(4″)); 3.28 (*s*, Me–C(8)); 3.03 (*s*, Me–C(4)). ^{13}C-NMR (150 MHz, $CDCl_3$): 187.12 (*d*, OH*C*–C(1)); 149.47 (*s*, C(6)); 148.19 (*s*, C(8)); 148.10 (*s*, C(4)); 143.39 (*s*, C(1′)); 142.78 (*s*, C(3a)); 141.40 (*s*, C(4′)); 140.10 (*s*, C(1″)); 138.82 (*d*, C(2)); 137.18 (*s*, C(8a)); 132.30 (*d*, C(7)); 130.98 (*d*, C(5)); 130.58 (*s*, C(1)); 129.11 (*d*, C(2′,6′)); 128.92 (*d*, C(3″,5″)); 127.76 (*d*, C(4″)); 127.58 (*d*, C(3′,5′)); 127.09 (*d*, C(2″,6″)); 117.62 (*d*, C(3)); 31.22 (*q*, *Me*–C(8)); 26.48 (*q*, *Me*–C(4)). EI-MS: 336 (100, $M^{+\bullet}$), 321 (50, $[M-Me]^+$), 319 (43, $[M-(Me+2\,H)]^+$), 293.2 (18, $[M-(CO+Me)]^+$), 292.2 (12, $[M-(CO+Me+H)]^{+\bullet}$), 291.1 (24, $[M-(CO+Me+2\,H)]^+$), 289.0 (21), 215.0 (32), 168.2 (27), 152.1 (43), 115.1 (25), 77.1 (58). Anal. calc. for $C_{25}H_{20}O$ (336.43): C 89.25, H 5.99; found: C 89.60, H 6.23.

1.4.3. *Azulene* **1f**. Yield of $NaBH_4$ reduction: 87%. Blue crystals. M.p. 166–167°. R_f (hexane/Et_2O 9:1) 0.62. IR (KBr): 3098*w*, 3056*w*, 3029*m*, 1571*s*, 1528*s*, 1486*s*, 1440*w*, 1396*m*, 1204*m*, 1038*m*, 834*s*, 766*s*, 691*s*. ^{1}H-NMR

(300 MHz, $CDCl_3$): 7.70 (*s*, H–C(2′,3′,5′,6′)); 7.67 (*dd*-like, $J_o = 7.1$, $J_m = 1.5$, H–C(2″,6″), H–C(2)); 7.54–7.30 (*m*, H–C(3″,4″,5″), H–C(3)); 7.20 (br. *s*, H–C(5,7)); 3.11 (*s*, Me–C(8)); 2.92 (*s*, H–C(1)); 2.91 (*s*, Me–C(4)). EI-MS ($C_{25}H_{22}$; 322.45): 322.0 (70, $M^{+\bullet}$), 307 (15, $[M - Me]^+$).

2. Thermal Reaction of Azulenes 1 with Dimethyl Acetylenedicarboxylate (ADM). – 2.1. *Reaction of 6-(*tert*-Butyl)-1,4,8-trimethylazulene* (**1a**). 2.1.1. *In MeCN*. The azulene (2.10 g, 9.29 mmol) and ADM (3.41 ml, 27.8 mmol), in MeCN (34 ml) were degassed and heated under Ar in a closed 50-ml *Schlenk* vessel at 110° during 24 h. The solvent was distilled off in a rotatory evaporator, and the residual dark yellow oil was dried under high vacuum to remove the rest of ADM. The residue was then subjected to CC (silica gel; hexane/Et_2O 4:1). Eight products were isolated as described below.

2.1.1.1. *Tetramethyl* trans-*6-(*tert*-Butyl)-2,4a-dihydro-3,8,9-trimethylphenanthrene-1,2,4,4a-tetracarboxylate* (*trans*-**6a**)[12]. Yield 0.05 g (1%). Pale yellow crystals. M.p. 187–188° (Et_2O/CH_2Cl_2). R_f (hexane/Et_2O 1:1) 0.24. UV/VIS (hexane): λ_{max} 339.7 (3.49), 242.7 (3.98); λ_{min} 293.5 (3.12), 226.9 (3.90). ^{1}H-NMR (600 MHz, $CDCl_3$): 7.10 (*d*, $^4J = 2.3$, H–C(5)); 7.01 (*d*, $^4J = 2.2$, H–C(7)); 6.86 (*quint.*-like, $^4J = 1.3$, H–C(10)); 4.28 (*s*, H–C(2)); 3.76 (*s*, MeOCO–C(4)); 3.73 (*s*, MeOCO–C(1)); 3.62 (*s*, MeOCO–C(2)); 3.46 (*s*, MeOCO–C(4a)); 2.49 (*s*, Me–C(8)); 2.32 (*s*, Me–C(9)); 2.21 (*s*, Me–C(3)); 1.23 (*s*, *t*-Bu). ^{13}C-NMR (150 MHz, $CDCl_3$): 172.93 (*s*, MeO*C*O–C(2)); 169.96 (*s*, MeO*C*O–C(4a)); 168.39(*s*, MeO*C*O–C(4)); 165.40 (*s*, MeO*C*O–C(1)); 149.02 (*s*, C(6)); 148.11 (*s*, C(1)); 140.63 (*s*, C(9)); 140.09 (*s*, C(4)); 136.29 (*s*, C(4b)); 133.93 (*s*, C(8)); 132.61 (*s*, C(8a)); 128.65 (*d*, C(7)); 125.83 (*s*, C(3)); 125.00 (*d*, C(10)); 120.77 (*d*, C(5)); 117.49 (*s*, C(10a)); 58.98 (*s*, C(4a)); 52.93 (*q*, *Me*OCO–C(2)); 52.53 (*q*, *Me*OCO–C(4a)); 51.96 (*q*, *Me*OCO–C(4)); 51.75 (*q*, *Me*OCO–C(1)); 51.44 (*d*, C(2)); 34.53 (*s*, Me_3C); 31.10 (*q*, Me_3C); 23.78 (*q*, *Me*–C(8)); 23.50 (*q*, *Me*–C(9)); 20.91 (*q*, *Me*–C(3)). CI-MS ($C_{29}H_{34}O_8$; 510.54): 528.1 (17, $[M + NH_4]^+$), 511.1 (8, $[M + H]^+$), 479.1 (12, $[M - MeO]^+$), 468 (10), 269 (11), 225 (8), 216 (77).

The structure of *trans*-**6a** was established by X-ray crystal-structure analysis (*cf. Fig. 4* and *Table 5*).

2.1.1.2. *Tetramethyl* endo-*10-(*tert*-Butyl)-2,8,12-trimethyltetracyclo[6.4.1.1^{2,5}.0^{5,13}]tetradeca-1(13),3,6,9,11-pentaene-3,4,6,7-tetracarboxylate* (*endo*-**3a**)[12]. Yield 0.430 g (9%). Yellow microcrystalline powder. M.p. 69–71°. R_f (hexane/Et_2O 1:1) 0.36. ^{1}H-NMR (600 MHz, $CDCl_3$): 6.15 (*s*, H–C(11)); 5.43 (*s*, H–C(9)); 3.89 (*s*, MeOCO–C(7)); 3.84 (*s*, MeOCO–C(3)); 3.73 (*s*, MeOCO–C(6)); 3.68 (*s*, MeOCO–C(4)); 2.74 (*d*, $^2J = 6.4$, H_a–C(14)); 2.28 (*d*, $^2J = 6.4$, H_s–C(14))[13]; 2.07 (*s*, Me–C(12)); 1.59 (*s*, Me–C(2)); 1.06 (*s*, Me_3C); 0.98 (*s*, Me–C(8)). ^{13}C-NMR (150 MHz, $CDCl_3$): 166.27 (*s*, MeO*C*O–C(3)); 165.98 (*s*, MeO*C*O–C(7)); 164.02 (*s*, MeO*C*O–C(6)); 163.56 (*s*, MeO*C*O–C(4)); 159.01 (*s*, C(13)); 155.90 (*s*, C(3)); 155.32 (*s*, C(7)); 148.89 (*s*, C(4)); 144.95 (s, C(10)); 140.89 (*s*, C(1)); 132.95 (*s*, C(12)); 131.96 (*s*, C(6)); 126.71 (*d*, C(11)); 121.03 (*d*, C(9)); 83.96 (*t*, C(14)); 69.88 (*s*, C(5)); 65.41 (*s*, C(2)); 52.32 (*q*, *Me*OCO–C(7)); 52.01 (*q*, *Me*OCO–C(3)); 51.92 (*q*, *Me*OCO–C(6)); 51.88 (*q*, *Me*OCO–C(4)); 48.63 (*s*, C(8)); 36.12 (*s*, Me_3C); 30.33 (*q*, Me_3C); 21.49 (*q*, Me–C(12)); 19.11 (*q*, *Me*–C(8)); 16.00 (*q*, Me–C(2)). GC/MS ($C_{29}H_{34}O_8$; 510.58): 510.2 (2, $M^{+\bullet}$), 495.2 (100, $[M - Me]^+$), 478.1 (60, $[M - MeOH]^{+\bullet}$), 463.1 (46, $[M - (Me + MeOH)]^+$), 422.1 (71), 421.1 (93, $[M - (MeOCO + 2\,Me)]^+$), 419.1 (50, $[M - 2\,MeOCO]^{+\bullet}$), 363.1 (96), 331.0 (54), 279.0 (68).

See *Fig. 3* for the AM1-calculated structure of *endo*-**3a**.

2.1.1.3. *Tetramethyl* exo-*10-(*tert*-Butyl)-2,8,12-trimethylpentacyclo[6.4.1.1^{2,5}.0^{5,13}.0^{9,13}]tetradeca-1(12),3,6,10-tetraene-3,4,6,7-tetracarboxyla te* (*exo*-**4a**)[12]. Yield 0.040 g (0.8%). Colorless crystals. M.p. 127° (hexane/CH_2Cl_2). R_f (hexane/Et_2O 1:1) 0.31. ^{1}H-NMR (600 MHz, $CDCl_3$): 5.79 (*s*, H–C(11)); 3.86 (*s*, MeOCO–C(7)); 3.80 (*s*, MeOCO–C(3)); 3.71 (*s*, MeOCO–C(4)); 3.60 (*s*, MeOCO–C(6)); 2.63 (*d*, $^2J = 8.1$, H_a–C(14)); 2.23 (*s*, H–C(9)); 2.03 (*s*, Me–C(12)); 1.87 (*d*, $^2J = 8.1$, H_s–C(14))[13]; 1.73 (*s*, Me–C(2)); 1.10 (*s*, Me_3C); 0.78 (*s*, Me–C(8)). ^{13}C-NMR (150 MHz, $CDCl_3$): 165.65 (*s*, MeO*C*O–C(7)); 165.50 (*s*, MeO*C*O–C(3)); 163.90 (*s*, MeO*C*O–C(4)); 163.58 (*s*, MeO*C*O–C(6)); 153.61 (*s*, C(7)); 148.01 (*s*, C(3)); 143.34 (*s*, C(10)); 142.35 (*s*, C(4)); 133.56 (*s*, C(6)); 128.78 (*s*, C(1)); 126.97 (*s*, C(12)); 125.52 (*d*, C(11)); 72.61 (*t*, C(14)); 66.60 (*s*, C(5)); 57.45 (*s*, C(2)); 52.17 (*q*, *Me*OCO–C(7)); 52.11 (*s*, C(13)); 52.01 (*q*, *Me*OCO–C(3)); 51.78 (*q*, *Me*OCO–C(4)); 51.69 (*q*, *Me*OCO–C(6)); 37.11 (*d*, C(9)); 35.48 (*q*, Me_3C); 28.89 (*q*, Me_3C); 22.68 (*s*, C(8)); 17.86 (*q*, *Me*–C(12)); 16.59 (*q*, *Me*–C(2)); 8.53 (*q*, *Me*–C(8)). Anal. calc. for $C_{29}H_{34}O_8$ (510.58): C 68.22, H 6.71; found: C 67.89, H 6.86.

The structure of *exo*-**4a** was established by an X-ray crystal-structure analysis (*cf. Fig. 1* and *Table 5*).

---

[12]) See *Scheme 2* for relative configurations.

[13]) H_a = *pro-S* and H_s = *pro-R* H-atom according to the defined relative configurations[12]).

2.1.1.4. *Dimethyl 8-(*tert-*Butyl)-1,6,10-trimethylheptalene-4,5-dicarboxylate* (**2a**) (*cf.* [26]). Yield 0.96 g (28%). Pale yellow crystals. M.p. 136.5–137.8° ([26]: 135–137°). R_f (hexane/Et_2O 1:1) 0.50. UV/VIS: see *Table 4* and *Fig. 9*.

A new X-ray crystal-structure analysis of **2a** was performed (see *Tables 3* and *5*); see [26] for a previous X-ray crystal-structure determination of **2a**.

2.1.1.5. *Dimethyl 6-(*tert-*Butyl)-4,8-dimethylazulene-1,2-dicarboxylate* (**11a**; *cf.* [26]). Yield 0.020 g (0.6%). Dark blue crystals. M.p. 114.7–116.0° ([26]: 122–123°). R_f (hexane/Et_2O 1:1) 0.42. ^{1}H-NMR (300 MHz, $CDCl_3$): 7.71 (*s*, H–C(2)); 7.40, 7.38 (2*s*, H–C(5,7)); 4.00 (*s*, MeOCO–C(2)); 3.93 (*s*, MeOCO–C(1)); 2.94 (*s*, Me–C(8)); 2.91 (*s*, Me–C(4)); 1.45 (*s*, Me_3C).

2.1.1.6. *Dimethyl (*Z*)-1-[6-(*tert-*Butyl)-1,4,8-trimethylazulen-3-yl]ethene-1,2-dicarboxylate* ((*Z*)-**10a**; *cf.* [11][26]). Yield 0.040 g (1%). Greenish-brown solid. M.p. 120.8–121.6°. R_f (hexane/Et_2O 1:1) 0.48. ^{1}H-NMR (300 MHz, $CDCl_3$): 7.52 (*s*, H–C(2′)); 7.18, 7.17 (2*s*, H–C(5′,7′)); 5.63 (*s*, H–C(2)); 3.92 (*s*, MeOCO–C(2)); 3.77 (*s*, MeOCO–C(1)); 3.04 (*s*, Me–C(4)); 2.86 (*s*, Me–C(8)); 2.78 (*s*, Me–C(1)); 1.42 (*s*, Me_3C).

2.1.1.7. *Tetramethyl* syn-*6-(*tert-*Butyl)-2,4,8-trimethyltetracyclo[6.3.3.0^{3,12}.0^{11,12}]tetradeca-2,4,6,9,13-pentaene-9,10,13,14-tetracarboxylate* (*syn*-**8a**)[12]. Yield 0.023 g (0.5%). R_f (hexane/AcOEt 1:1) 0.65. For further data, see *2.2.4*.

2.1.1.8. *Tetramethyl 2,6-Dimethylazulene-4,5,7,8-tetracarboxylate* (**9**). Yield 0.005 g (0.2%). R_f (hexane/AcOEt 1:1) 0.43. For further data, see *2.2.5*.

2.1.2. *In DMF.* The azulene (0.100 g, 0.44 mmol) and ADM (0.16 ml, 1.32 mmol) in DMF (5 ml) were degassed with Ar and heated in a closed 10-ml *Schlenk* vessel at 110° during 24 h. Workup as described gave a dark yellow oil, which was subjected to CC (silica gel; hexane/Et_2O 4:1). With the exception of (*Z*)-**10a**, the same products as decribed under *2.1.1* were isolated in similar ratios.

2.2. *Reaction of 6-(*tert-*Butyl)-1,4,8-trimethyl[3-^{2}H]azulene* ([3-^{2}H]-**1a**). The partially labeled azulene (0.300 g, 1.31 mmol) and ADM (0.48 ml, 3.92 mmol) in MeCN (5.0 ml) were degassed with Ar and heated in a closed 10-ml *Schlenk* vessel at 110° during 24 h. The usual workup, followed by CC (silica gel; hexane/Et_2O 4:1 to 1:1), was performed. The following nine products were isolated:

2.2.1. *Tetramethyl* trans-*6-(*tert-*Butyl)-2,4a-dihydro-3,8,9-trimethyl[2-^{2}H]phenanthrene-1,2,4,4a-tetracarboxylate* (*trans*-[2-^{2}H]-**6a**). ^{1}H-NMR (300 MHz, $CDCl_3$): 4.28 (*s*, H–C(2); residual H 35%)[14]. ^{2}H-NMR (92 MHz, $CDCl_3$): 4.28 (br. *s*, ^{2}H–C(2)).

2.2.1.1. *Tetramethyl 6-(*tert-*Butyl)-1,2-dihydro-3,8,9-trimethyl[1-^{2}H]phenanthrene-1,2,2,4-tetracarboxylate* ([1-^{2}H]-**7a**). Heating of *trans*-**6a** in MeCN (*c* = *ca.* 0.25 M) at 110° for 3 h led quantitatively to [1-^{2}H]-**7a** (UV evidence; see 2.2.6).

2.2.2. *Tetramethyl* endo-*10-(*tert-*Butyl)-2,8,12-trimethyl[14-^2H_a]tetracyclo[6.4.1.1^{2,5}.0^{5,13}]-tetradeca-1(13),3,6,9,11-pentaene-3,4,6,7-tetracarboxylate* (*endo*-[14-^2H_a]-**3a**). ^{1}H-NMR (300 MHz, $CDCl_3$): 2.74 (*d*, H_a–C(14); residual H 9%); 2.28 (*s*, H_s–C(14)). ^{2}H-NMR (92 MHz, $CDCl_3$): 2.74 (br. *s*, ^2H_a–C(14)).

2.2.3. *Tetramethyl* exo-*10-(*tert-*Butyl)-2,8,12-trimethyl[14-^2H_s]pentacyclo[6.4.1.1^{2,5}.0^{5,13}.0^{9,13}]tetradeca-1(12),3,6,10-tetraene-3,4,6,7-tetracarboxylate* (*exo*-[14-^2H_s]-**4a**): ^{1}H-NMR (300 MHz, $CDCl_3$): 1.88 (*d*, H_s–C(14); residual H 22%); 2.64 (*s*, H_a–C(14)). ^{2}H-NMR (92 MHz, $CDCl_3$): 1.88 (br. *s*, ^2H_s–C(14)).

2.2.4. *Tetramethyl* syn-*6-(*tert-*Butyl)-2,4,8-trimethyl[11-^{2}H]tetracyclo[6.3.3.0^{3,12}.0^{11,12}]tetradeca-2,4,6,9,13-pentaene-9,10,13,14-tetracarboxylate* (*syn*-[11-^{2}H]-**8a**). Yield 0.014 g (3%). Colorless crystals. M.p. 199.3–199.6° (Et_2O). UV/VIS (MeCN): λ_{max} 343 (sh, 3.32), 290.5 (3.85) 215.3 (4.41); λ_{min} 269 (3.76). ^{1}H-NMR (300 MHz, $CDCl_3$): 6.03 (*s*, H–C(7)); 5.72 (*s*, H–C(5)); 4.04 (*s*, H–C(1)); 3.89 (*s*, MeOCO–C(13)); 3.74 (*s*, MeOCO–C(14); 3.70 (*s*, MeOCO–C(9)); 3.67 (*s*, MeOCO–C(10)); 3.31 (*s*, H–C(11); *ca.* 3% H); 2.20 (*s*, Me–C(4)); 2.12 (*s*, Me–C(2)); 1.32 (*s*, Me–C(8)); 1.06 (*s*, Me_3C). ^{2}H-NMR (92 MHz, $CDCl_3$): 3.31 (br. *s*, ^{2}H–C(11)). CI-MS ($C_{29}H_{33}{}^2HO_8$; 511.58): 529.1 (17, $[M+NH_4]^+$), 512.1 (3, $[M+H]^+$), 500.0 (3), 497.1 (3), 481.0 [2, $[(M+1)-MeO]^{+\cdot}$), 480.0 (8, $[(M+1)-MeOH]^{+\cdot}$).

The structure was established by an X-ray crystal-structure analysis (*cf. Fig. 7* and *Table 5*).

2.2.5. *Tetramethyl 2,6-Dimethyl[1-^{2}H]azulene-4,5,7,8-tetracarboxylate* ([1-^{2}H]-**9**). Yield 0.006 (1%). Blue crystals. M.p.192.1–192.3° (Et_2O). R_f (hexane/AcOEt 1:1) 0.43. UV/VIS (MeCN): λ_{max} 585 (3.27), 369.2 (4.08), 352.7 (4.05), 325.9 (4.29), 299.1 (5.17), 288 (sh, 5.04), 259.2 (4.64); λ_{min} 495 (3.25), 359.5 (4.03), 343.8 (4.02), 320.0 (4.27), 269.9 (4.60), 241.7 (4.60). ^{1}H-NMR (600 MHz, $CDCl_3$): 7.27 (*s*, H–C(3); 1.05 H, *i.e.*, *ca.* 1.0 ^{2}H–C(1)); 4.00 (*s*, 2 MeOCO–C(4,8)); 3.91 (*s*, 2 MeOCO–C(5,7)); 2.62 (*s*, Me–C(2)); 2.53 (*s*, Me–C(6)).

---

[14] Limit of integration ≥3%.

^{13}C-NMR (150 MHz, $CDCl_3$): 169.78 (*s*, MeO*C*O–C(4,8)); 168.67 (*s*, MeO*C*O–C(5,7)); 154.01 (*s*, C(2)); 140.07 (*s*, C(6)); 136.19/136.15 (*s*, C(5,7)); 135.27/135.22 (*s*, C(4,8)); 128.38 (*s*, C(3a,8a)); 123.08 (*s*, C(1,3)); 53.11 (*q*, *Me*OCO–C(5,7)); 52.87 (*q*, *Me*OCO–C(4,8)); 24.69 (*q*, *Me*–C(6)); 16.87 (*q*, *Me*–C(2)). GC/MS ($C_{20}H_{19}{}^2HO_8$; 389.37): 390.1 (30, $[M+H]^+$), 389.0 (83, $M^{+\cdot}$), 358 (66, $[M-MeO]^+$), 343.0 (57, $[M-(MeO+Me)]^{+\cdot}$), 342.0 (100, $[M-(MeOH+Me)]^+$), 271 (79, $[M-2\,MeOCO]^{+\cdot}$), 227 (49).

The structure of [1-^{2}H]-**9** was established by an X-ray crystal-structure analysis (*cf. Fig. 6* and *Table 5*).

2.2.6. *Tetramethyl 6-(*tert-*Butyl)-1,2-dihydro-3,8,9-trimethyl[1-^{2}H]phenanthrene-1,2,2,4-tetracarboxylate* ([1-^{2}H]-**7a**). Yield 0.004 g (0.6%). Colorless crystals. M.p. 213.2–214.6° (CH_2Cl_2/Et_2O). UV/VIS (hexane/i-PrOH 95:5): λ_{max} 343 (sh, 0.18), 327 (0.25), 252 (1.00), 226 (0.66); λ_{min} 281 (0.07), 234 (0.62). ^{1}H-NMR (300 MHz, $CDCl_3$): 7.56 (*s*, H–C(5)); 7.26 (*s*, H–C(10)); 7.16 (*s*, H–C(7)); 4.41 (*s*, H–C(1); residual H 12.5%); 3.84 (*s*, MeOCO–C(2)); 3.68 (*s*, MeOCO–C(1)); 3.62 (*s*, MeOCO–C(4)); 3.48 (*s*, MeOCO–C(2)); 2.88 (*s*, Me–C(9)); 2.86 (*s*, Me–C(8)); 2.29 (*s*, Me–C(3)); 1.34 (*s*, Me_3C). GC/MS ($C_{29}H_{33}{}^2HO_8$; 511.58): 512.1 (11, $[M+H]^+$), 511.1 (30, $M^{+\cdot}$), 510.1 (9, $[M-1]^{+\cdot}$), 479.1 (22, $[M-MeOH]^{+\cdot}$), 420.1 ($M-(MeOCO+MeOH)]^+$), 419.1 ($M-(MeOCO+MeO[^2H])]^+$), 331.0 (100, $[M-2\,(MeOCO+MeO)]^{+\cdot}$).

The structure was established by an X-ray crystal-structure analysis (*cf. Fig. 5* and *Table 5*).

2.2.7. *Dimethyl 8-(*tert-*Butyl)-1,6,10-trimethyl[3-^{2}H]heptalene-4,5-dicarboxylate* ([3-^{2}H]-**2a**). Yield 0.140 g (29%). ^{1}H-NMR (300 MHz, $CDCl_3$): 7.51 (*d*, $^3J=6$, H–C(2); residual H 12%); 6.27 (*s*, H–C(3)). GC/MS ($C_{23}H_{27}{}^2HO_4$; 369.48): 369.1 (100, $M^{+\cdot}$), 354.1 (32, $[M-Me]^+$), 322.1 (32, $[M-(Me+MeOH)]^+$), 287.0 (33, $[M-Me_3CC{\equiv}CH]^{+\cdot}$), 284.0 (10, $[M-[^2H]C{\equiv}CE_{Me}]^{+\cdot}$), 271.1 (37, $[M-MeC{\equiv}CE_{Me}]^{+\cdot}$), 227.1 (84, $[M-ADM]^{+\cdot}$).

2.2.8. *Dimethyl 6-(*tert-*Butyl)-4,8-dimethyl[3-^{2}H]azulene-1,2-dicarboxylate* ([3-^{2}H]-**11a**). Yield 0.002 g (0.4%). ^{1}H-NMR (300 MHz, $CDCl_3$): 7.71 (*s*, H–C(3); residual H *ca.* 20%).

2.2.9. *Dimethyl (Z)-1-[6-(*tert-*Butyl)-1,4,8-trimethylazulen-3-yl]ethene-1,2-dicarboxylate* ((*Z*)-**10a**). Yield 0.003 g (0.6%).

2.3. *Reaction of 1,4,6,8-Tetramethylazulene* (**1b**). The azulene (1.00 g, 5.43 mmol) and ADM (2.00 ml, 16.29 mmol) in MeCN (20 ml) were degassed with Ar and heated in a closed 50-ml *Schlenk* vessel at 110° during 24 h. The solvent was distilled off, and the yellow residue was subjected to CC (silica gel; hexane/Et_2O 4:1). The following six products were isolated and characterized.

2.3.1. *Tetramethyl* trans-*2,4a-dihydro-3,6,8,9-tetramethylphenanthrene-1,2,4,4a-tetracarboxylate* (*trans*-**6b**)[12]). Yield 0.10 g (4%). Light yellow crystals. M.p. 187.7–188.8°. IR (KBr): 3414*m*, 2954*w*, 1740*s* ,1695*s* , 1636*s*, 1609*s*, 1432*s* , 1385*m*, 1307*s*, 1207*s*, 1107*s*, 1057*w*, 985*w*, 878*w*, 820*m*, 788*m*. ^{1}H-NMR (600 MHz, $CDCl_3$): 6.87 (*quint*-like *s*, H–C(10)); 6.85 (br. *s*, H–C(7)); 6.82 (br. *s*, H–C(5)); 4.29 (*s*, H–C(2)); 3.77 (*s*, MeOCO–C(4)); 3.73 (*s*, MeOCO–C(1)); 3.62 (*s*, MeOCO–C(2)); 3.51 (*s*, MeOCO–C(4a)); 2.44 (*s*, Me–C(8)); 2.31 (*s*, Me–C(9)); 2.23 (*s*, Me–C(3,6)). ^{13}C-NMR (150 MHz, $CDCl_3$): 173.00 (*s*, MeO*C*O–C(2)); 170.11 (*s*, MeO*C*O–C(4a)); 168.36 (*s*, MeO*C*O–C(4)); 165.41 (*s*, MeO*C*O–C(1)); 147.99 (*s*, C(1)); 140.65 (*s*, C(9)); 136.56 (*s*, C(4b)); 135.99 (*s*, C(4)); 134.39 (*s*, C(8)); 132.72 (*s*, C(7,8a)); 125.72 (*s*, C(3)); 124.86 (*s*, C(10)); 123.90 (*d*, C(5)); 117.62 (*s*, C(10a)); 58.57 (*s*, C(4a)); 52.98 (*q*, *Me*OCO–C(2)); 52.55 (*q*, *Me*OCO–C(4a)); 52.00 (*q*, *Me*OCO–C(4)); 51.76 (*q*, *Me*OCO–C(1)); 51.42 (*d*, C(2)); 23.52 (*q*, *Me*–C(9)); 23.40 (*q*, *Me*–C(8)); 21.27 (*q*, *Me*–C(6)); 21.05 (*q*, *Me*–C(3)). EI-MS: 468.2 (32, $M^{+\cdot}$), 436.2 (18.5, $[M-MeOH]^{+\cdot}$), 409.2 (24.5, $[M-MeOCO]^+$), 377.2 (100.0, $[M-(MeOCO+MeOH)]^+$), 365.2 (47, $[M-(MeOCO+CO_2]^+$), 350.2 (50, $[M-2\,MeOCO]^{+\cdot}$), 333.2 (52), 276.1 (61), 141.9 (44). Anal. calc. for $C_{26}H_{28}O_8$ (468.50): C 66.65, H 6.02; found: C 66.44, H 6.11.

2.3.2. *Tetramethyl* endo-*2,8,10,12-Tetramethyltetracyclo[6.4.1.1^{2,5}.0^{5,13}]tetradeca-1(13),3,6,9,11-pentaene-3,4,6,7-tetracarboxylate* (*endo*-**3b**)[12]). Yield 0.050 g (2%). Isolated as *ca.* 1:1 mixture with *exo*-**4b**. ^{1}H-NMR (300 MHz, $CDCl_3$): 6.58 (*s*, H–C(11)); 5.30 (*s*, H–C(9)).

2.3.3. *Tetramethyl* exo-*2,8,10,12-Tetramethylpentacyclo[6.4.1.1^{2,5}.0^{5,13}.0^{9,13}]tetradeca-1(12),3,6,10-tetraene-3,4,6,7-tetracarboxylate* (*exo*-**4b**)[12]). Yield 0.025 g (1%). Isolated as *ca.* 1:1 mixture with *endo*-**3b**. ^{1}H-NMR (300 MHz, $CDCl_3$): 5.87 (*s*, H–C(11)).

2.3.4. *Dimethyl 1,6,8,10-Tetramethylheptalene-4,5-dicarboxylate* (**2b**; *cf.* [28]). Yield 0.55 g (31%).

2.3.5. *Dimethyl 4,6,8-Trimethylazulene-1,2-dicarboxylate* (**11b**; *cf.* [28]). Only trace yield.

2.3.6. *Dimethyl (Z)-(1,4,6,8-Tetramethylazulen-3-yl)ethene-1,2-dicarboxylate* ((*Z*)-**10b**; *cf.* [11][28]). Yield 0.011 g (0.6%).

2.4. *Base-Catalyzed Reaction of* trans-**6b**. Na (*ca.*1 mg) was dissolved in MeOH (2.0 ml), and *trans*-**6b** (8 mg, 0.017 mmol) was added. The soln. was heated at 40° during 3 h. Then, cold H_2O (5 ml) was added, and the soln. was acidified with 1N aq. HCl and extracted with Et_2O (20 ml). The org. phase was washed with 1N aq. HCl and

then with brine. After drying ($MgSO_4$), the solvent was distilled off. Three products were separated by prep. HPLC (column: *Spherisorb CN* (5 μm; 250 × 20 mm); eluant: hexane/i-PrOH 95:5; flow rate: 0.8 ml/min).

2.4.1. *Trimethyl* trans-*1,4-Dihydro-3,6,8,9-tetramethylphenanthrene-1,2,4-tricarboxylate* (**18b**). t_R (see *2.4.*) 5.35 min. UV/VIS (hexane/i-PrOH 95:5): λ_{max} 330 (<0.01), 310 (sh, 0.09), 292.5 (0.12), 280 (sh, 0.11), 247 (1.00), 243 (0.98); λ_{min} 325 (<0.01), 258 (0.06), 245 (0.97). ^{1}H-NMR (600 MHz, $CDCl_3$): 7.63 (*s*, H–C(5)); 7.33 (*s*, H–C(10)); 7.12 (*s*, H–C(7)); 5.04 (*s*, H–C(1)); 4.99 (*s*, H–C(4)); 3.83 (*s*, MeOCO–C(2)); 3.64 (*s*, MeOCO–C(1)); 3.56 (*s*, MeOCO–C(4)); 2.92 (*s*, Me–C(9)); 2.89 (*s*, Me–C(8)); 2.51 (*s*, Me–C(3)); 2.46 (*s*, Me–C(6)). ^{13}C-NMR (150 MHz, $CDCl_3$): 171.11 (*s*, MeO*C*O–C(1)); 170.44 (*s*, MeO*C*O–C(4)); 167.27 (*s*, MeO*C*O–C(2)); 145.64 (*s*, C(3)); 136.16 (*s*, C(8)); 135.57 (*s*, C(6)); 135.51 (*s*, C(9)); 132.93 (*s*, C(4b)); 131.84 (*d*, C(7)); 130.80 (*s*, C(8a)); 129.73 (*d*, C(10)); 129.26 (*s*, C(10a)); 125.36 (*s*, C(4a)); 124.21 (*s*, C(2)); 121.15 (*d*, C(5)); 53.08 (*d*, C(4)); 52.58 (*q*, *Me*OCO–C(4)); 52.41 (*q*, *Me*OCO–C(1)); 51.88 (*q*, *Me*OCO–C(2)); 48.69 (*d*, C(1)); 26.26 (*q*, *Me*–C(9)); 26.12 (*q*, *Me*–C(8)); 21.63 (*q*, *Me*–C(6)); 21.51 (*q*, *Me*–C(3)). GC/MS ($C_{24}H_{26}O_6$; 410.46): 411.1 (9, $[M+H]^+$), 410.1 (34, $M^{+\cdot}$), 351.1 (11, $[M-MeOCO]^+$), 320.1 (21, $[(M+H)-(MeOCO+MeOH)]^{+\cdot}$), 319.1 (96, $[M-(MeOCO+MeOH)]^+$), 307.1 (30, $[M-(MeOCO+CO_2)]^+$), 292.1 (63, $[M-2\,MeOCO]^{+\cdot}$), 275.1 (35, $[M-MeOCO+CO_2+MeOH)]^+$), 249.1 (20, $[(M+H)-(2\,MeCO+CO_2)]^+$), 248.1 (100, $[M-(2\,MeOCO+CO_2)]^{+\cdot}$).

2.4.2. *Tetramethyl 1,2-Dihydro-3,6,8,9-tetramethylphenanthrene-1,2,2,4-tetracarboxylate* (**7b**). t_R (see *2.4.*) 6.07 min. UV/VIS (hexane/i-PrOH 95:5): λ_{max} 385 (0.06), 364 (0.06), 314 (sh, 0.26), 274 (1.00), 258 (sh, 0.78), 233.5 (0.75); λ_{min} 370 (0.05), 347 (0.04), 245 (0.70). ^{1}H-NMR (600 MHz, $CDCl_3$): 7.39 (s, H–C(5)); 7.15 (s, H–C(10)); 7.04 (s, H–C(7)); 4.44 (s, H–C(1)); 3.84 (s, MeOCO–C(2)); 3.68 (s, MeOCO–C(1)); 3.63 (s, MeOCO–C(4)); 3.48 (s, MeOCO–C(2)); 2.86 (s, Me–C(9)); 2.84 (s, Me–C(8)); 2.37 (s, Me–C(6)); 2.29 (s, Me–C(3)). ^{13}C-NMR (150 MHz, $CDCl_3$): 170.24 (s, MeOCO–C(4)); 170.14 (s, MeOCO–C(1)); 169.16 (s, MeO*C*O–C(2)); 168.82 (*s*, MeO*C*O–C(2)); 138.33 (*s*, C(3)); 136.83 (*s*, C(9)); 135.86 (*s*, C(8)); 134.92 (*s*, C(6)); 132.33 (*s*, C(10a)); 131.79 (*s*, C(8a)); 131.72 (*d*, C(7)); 129.05 (*s*, C(4b)); 128.83 (*s*, C(4)); 128.13 (*d*, C(10)); 128.11 (*s*, C(4a)); 122.55 (*d*, C(5)); 63.47 (*s*, C(2)); 53.42 (*q*, *Me*OCO–C(2)); 53.17 (*q*, *Me*OCO–C(2)); 52.27 (*q, Me*OCO–C(1)); 51.97 (*q*, *Me*OCO–C(4)); 51.39 (*d*, C(1)); 26.16 (*q*, *Me*–C(9)); 26.04 (*q*, *Me*–C(8)); 21.27 (*q*, *Me*–C(6)); 18.66 (*q*, *Me*–C(3)). GC/MS ($C_{26}H_{28}O_8$; 468.49): 469.1 (9, $[M+H]^+$), 468.1 (37, $M^{+\cdot}$), 437.1 (11, $[(M+H)-MeOH]^+$), 436.1 (30, $[M-MeOH)]^+$), 378.1 (24, $(M+H)-(MeOCO+MeOH)]^{+\cdot}$), 377.1 (100, $(M-(MeOCO+MeOH)]^+$), 345.0 ($M-(MeOCO+2\,MeOH)]^+$).

2.4.3. *Trimethyl 3,6,8,9-Tetramethylphenanthrene-1,2,4-tricarboxylate* (**19b**). t_R (see *2.4.*) 8.42 min. UV/VIS (hexane/i-PrOH 95:5): λ_{max} 348 (sh, 0.15), 326 (0.23), 313 (sh, 0.18), 251 (1.00); λ_{min} 290 (0.11), 233 (0.61). ^{1}H-NMR (600 MHz, $CDCl_3$): 8.04 (*s*, H–C(5)); 7.58 (*s*, H–C(10)); 7.29 (*s*, H–C(7)); 4.00 (*s*, MeOCO–C(1)); 3.95 (*s*, MeOCO–C(2)); 3.93 (*s*, MeOCO–C(4)); 2.90 (*s*, Me–C(8)); 2.89 (*s*, Me–C(9)); 2.51 (*s*, Me–C(3)); 2.47 (*s*, Me–C(6)). ^{13}C-NMR (150 MHz, $CDCl_3$): 171.80 (*s*, MeO*C*O–C(4)); 168.41 (*s*, MeO*C*O–C(2)); 168.24 (*s*, MeO*C*O–C(1)); 136.23 (*s*, C(9)); 135.85 (*s*, C(8)); 135.00 (*s*, C(6)); 134.11 (*d*, C(7)); 133.90 (*s*, C(2)); 133.31 (*s*, C(3)); 131.42 (*s*, C(8a)); 131.20 (*s*, C(4)); 130.21 (*s*, C(1)); 129.14(*s*, C(4a)); 125.00 (*d*, C(5)); 124.91 (*s*, C(4b)); 124.30 (*d*, C(10)); 124.12 (*s*, C(10a)); 53.05 (*q*, *Me*OCO–C(1)); 52.87 (*q*, *Me*OCO–C(2)); 52.80 (*q*, *Me*OCO–C(4)); 27.02 (*q*, Me–C(9)); 26.23 (*q*, Me–C(8)); 21.62 (*q*, Me–C(6)); 17.93 (*q*, Me–C(3)). GC/MS ($C_{24}H_{24}O_6$; 408.44): 408.1 (97, $M^{+\cdot}$), 377.1 (23, $[M-MeO]^+$), 361.1 (47, $[M-(Me+MeOH)]^+$), 290.1 (100, $[M-2\,MeOCO]^{+\cdot}$), 207.0 (97, $[M-(ADM+MeOCO)]^+$).

2.5. *Reaction of Guaiazulene* (**1c**; *cf.* [9]). The azulene (1.00 g, 5.04 mmol) and ADM (1.85 ml, 15.12 mmol) in MeCN (21 ml) were degassed with Ar and heated in a closed 50-ml *Schlenk* vessel at 110° during 24 h. The resulting dark yellow oil was dried under high vacuum to remove residual amounts of ADM, followed by CC (silica gel; hexane/Et_2O 4:1 to 1:1). Nine products were isolated, whereby the fraction of *endo*-**5c** and *exo*-**5c** was further separated by HPLC.

2.5.1. *Tetramethyl 1,2-Dihydro-7-isopropyl-3,9-dimethylphenanthrene-1,2,2,4-tetracarboxylate* (**7c**). Yield 0.007 g (0.3%). Colorless crystals. M.p. 187.2–187.9°. R_f (hexane/AcOEt 1:1) 0.50. ^{1}H-NMR (300 MHz, (D_6)acetone): 7.83 (*d*, J_m = 1.8, H–C(8)); 7.69 (*d*, J_o = 8.9, H–C(5)); 7.46 (*dd*, J_o = 8.9, J_m = 1.8, H–C(8)); 7.33 (*s*, H–C(10)); 4.39 (*s*, H–C(1)); 3.85 (*s*, MeOCO–C(2)); 3.68 (*s*, MeOCO–C(1)); 3.61 (*s*, MeOCO–C(4)); 3.43 (*s*, MeOCO–C(2)); 3.10 (*sept*. J_{VIC} = 6.9 Me_2CH); 2.67 (*s*, Me–C(9)); 2.23 (*s*, Me–C(3)); 1.33 (*d*, J_{VIC} = 6.9, Me_2CH). GC/MS ($C_{27}H_{30}O_8$; 482.52): 483.9 (10, $[M+1]^+$), 482.1 (32, $M^{+\cdot}$), 450.1 (70, $[M-MeOH]^{+\cdot}$), 391.1 (100, $[M-(MeOCO+MeOH]^+$), 359.0 (32, $[M-(MeOCO+2\,MeOH]^+$).

2.5.2. *Tetramethyl* syn-*5-Isopropyl-2,8-dimethyltetracyclo[6.3.3.0^{3,12}.0^{11,12}]tetradeca-2,4,6,9,13-pentaene-9,10,13,14-tetracarboxylate* (*syn*-**8c**)[12]). Yield 0.0195 g (0.8%). Yellow crystals. M.p. 149.6–150.1°. R_f (hexane/AcOEt 1:1) 0.34. UV/VIS (MeCN): λ_{max} 344 (sh, 3.40), 290 (sh, 3.74), 212 (4.41); λ_{min} *ca.* 276 (3.74). ^{1}H-NMR (300 MHz, $CDCl_3$): 6.35 (*d*, ^3J = 11.5, H–C(7)); 6.29 (*s*, H–C(4)); 5.67 (*d*, ^3J = 11.5, H–C(6)); 4.14 (*d*, ^3J = 1.5,

H–C(1)); 3.88 (*s*, MeOCO–C(13)); 3.71 (*s*, MeOCO–C(14)); 3.67 (*s*, MeOCO–C(9,10)); 3.30 (*d*, $^3J = 1.5$, H–C(11)); 2.39 (*sept.*, $J_{VIC} = 6.9$, Me_2CH); 2.04 (*s*, Me–C(2)); 1.33 (*s*, Me–C(8)); 1.06, 1.04 (2*d*, $J_{VIC} = 6.9/6.9$, Me_2CH). CI/MS ($C_{27}H_{30}O_8$; 482.52): 501 (31, $[(M+1)+NH_4]^+$), 500 (100 $[M+NH_4]^+$), 485 (12, $[(M+NH_4)-Me]^+$), 468 (7, $[(M+NH_4)-MeOH]^+$).

2.5.3. *Tetramethyl* exo-*8-Isopropyl-3a,6-dihydro-1,6-dimethyl-1,3a-methanophenalene-2,3,4,5-tetracarboxylate* (*exo*-**5c**)[12]. Yield 0.010 g (0.4%). Colorless oil. R_f (hexane/AcOEt 1:1) 0.40. t_R (see *2.4*) 8.11 min. ^{1}H-NMR (300 MHz, $CDCl_3$): 6.99 (*s*, H–C(9)); 6.73 (*s*, H–C(7)); 3.86 (*q*, $^3J = 7.1$, H–C(6)); 3.86 (*s*, MeOCO–C(4)); 3.780, 3.773 (2*s*, MeOCO–C(5,2)); 3.69 (*s*, MeOCO–C(3)); 2.92 (*d*, $^2J = 7.3$, H_a–C(10)); 2.88 (*sept.*, $J_{VIC} = 6.9$, Me_2CH); 2.22 (*d*, $^2J = 7.3$, H_s–C(10)); 1.71 (*s*, Me–C(1)); 1.43 (*d*, $^3J = 7.2$, Me–C(6)); 1.24 (*d*, $J_{VIC} = 6.9$, Me_2CH).

2.5.4. *Tetramethyl* endo-*8-Isopropyl-3a,6-dihydro-1,6-dimethyl-1,3a-methanophenalene-2,3,4,5-tetracarboxylate* (*endo*-**5c**)[12]. Yield 0.007 g (0.3%). Colorless oil. R_f (hexane/AcOEt 1:1) 0.40. R_t (see *2.4*) 9.46 min. ^{1}H-NMR (300 MHz, $CDCl_3$): 7.01 (*s*, H–C(9)); 6.80 (*s*, H–C(7)); 3.97 (*q*, $^3J = 7.3$, H–C(6)); 3.89 (*s*, MeOCO–C(4)); 3.775, 3.766 (2*s*, MeOCO–C(5,3)); 3.64 (*s*, MeOCO–C(2)); 3.17 (*d*, $^2J = 7.5$, H_a–C(10)); 2.90 (*sept;* $J_{VIC} = 6.9$, Me_2CH); 2.37 (*d*, $^2J = 7.5$, H_s–C(10)); 1.70 (*s*, Me–C(1)); 1.42 (*d*, $^3J = 7.3$, Me–C(6)); 1.251, 1.246 (2*d*, $J_{VIC} = 6.9$, 6.9, Me_2CH).

2.5.5. *Tetramethyl* exo-*11-Isopropyl-2,8-trimethylpentacyclo[6.4.1.1^{2,5}.0^{5,13}.0^{9,13}]tetradeca-1(12),3,6,10-tetraene-3,4,6,7-tetracarboxylate* (*exo*-**4c**)[12]. Isolated as a *ca.* 1:1 mixture with *exo*-**5c**. Yield 0.010 g (0.4%). R_f (hexane/AcOEt 1:1) 0.41. ^{1}H-NMR (600 MHz, $CDCl_3$): 6.05 (*s*, H–C(12)); 5.60 (*d*, $^3J = 4.6$, H–C(10)); 3.85 (*s*, MeOCO–C(7)); 3.77 (*s*, MeOCO–C(3)); 3.70 (*s*, MeOCO–C(4)); 3.61 (*s*, MeOCO–C(6)); 2.81 (*d*, $^2J = 8.2$, H_a–C(14)); 2.46 (*sept*, $J_{VIC} = 6.9$, Me_2CH); 2.30 (*d*, $^3J = 4.5$, H–C(9)); 1.91 (*d*, $^2J = 8.2$, H_s–C(14)); 1.57 (*s*, Me–C(2)); 1.07, 1.05 (2*d*, *J*vic = 6.8, 6.9, Me_2CH); 0.83 (*s*, Me–C(8)).

2.5.6. *Tetramethyl* endo-*11-Isopropyl-2,8-dimethyltetracyclo[6.4.1.1^{2,5}.0^{5,13}]tetradeca-1(13),3,6,9,11-pentaene-3,4,6,7-tetracarboxylate* (*endo*-**3c**)[12]. Yield 0.5%. Obtained only in a mixture with *trans*-**6c**.

2.5.7. *Dimethyl 9-Isopropyl-1,6-dimethylheptalene-4,5-dicarboxylate* (**2c**; *cf.* [9]). Yield 1.08 g (63%). Pale yellow crystals. M.p. 147° ([9]: 141–142.5°). R_f (hexane/Et_2O 1:1) 0.46.

2.5.8. *Tetramethyl* trans-*2,4a-Dihydro-7-isopropyl-3,9-trimethylphenanthrene-1,2,4,4a-tetracarboxylate* (*trans*-**6c**)[12]. Yield 0.008 g (0.3%). Obtained only in a mixture with *endo*-**3c**.

2.5.9. *Dimethyl (Z)-1-(7-Isopropyl-1,4-dimethylazulen-3-yl)ethene-1,2-dicarboxylate* ((*Z*)-**10c**; *cf.* [11]). Yield 0.016 g (0.9%).

2.5.10. *Reaction of* **1c** *and ADM in the Presence of Di([$^2H_3$]methyl) Carbonate.* The azulene (0.550 g, 2.78 mmol), ADM (1.02 ml), and di([$^2H_3$]methyl) carbonate (0.75 ml, 8.34 mmol) in MeCN (12 ml) were degassed with Ar and heated in a closed 50-ml *Schlenk* vessel at 110° during 24 h. Then, the described products were isolated by CC. Neither *trans*-**6c** nor **7c** showed any incorporation of [$^2H_3$]MeO groups in their ester parts.

2.6. *Reaction of 1,4,8-Trimethyl-6-phenylazulene* (**1d**). The azulene (0.300 g, 1.22 mmol) and ADM (0.45 ml, 3.66 mmol) in MeCN (10 ml) were degassed with Ar and heated in a closed 10-ml *Schlenk* vessel at 110° for 24 h. The deeply yellow colored residue was subjected to CC (silica gel; hexane/Et_2O 1:2). The following seven products were isolated and characterized.

2.6.1. *Dimethyl 1,6,10-Trimethyl-8-phenylheptalene-4,5-dicarboxylate* (**2d**). Yield 0.180 g (38%). Yellow crystals. M.p. 187–188°. R_f (hexane/Et_2O 1:1) 0.44. UV/VIS: see *Table 4* and *Fig. 10*. IR (KBr): 3004*w*, 2949*m*, 2908*w*, 1707*s*, 1642*m*, 1523*w*, 1438*s*, 1378*w*, 1307*s*, 1281*s*, 1266*s*, 1193*m*, 1052*s*, 866*m*, 771*m*. ^{1}H-NMR (600 MHz, C_6D_6): 7.72 (*dq*-like, $^3J = 5.9$, $^5J = 1.0$, H–C(3)); 7.47 (*dt*, $J_o = 7.1$, $J_m = 1.6$, H–C(2′,6′)); 7.16 (*t*, partly covered by C_6D_5H, H–C(3′,5′)); 7.10 (*tt*, $J_o = 7.3$, $J_m = 1.6$, H–C(4′)); 6.54 (*s*, H–C(9)); 6.35 (*quint*-like, $^4J = 1.3$, H–C(7)); 5.91 (*dq*-like, $^3J = 5.9$, $^4J = 1.3$, H–C(2)); 3.47 (*s*, MeOCO–C(5)); 3.26 (*s*, MeOCO–C(4)); 2.03 (*d*, $^4J = 1.3$, Me–C(6)); 1.76 (*t*-like, $^4J \approx {}^5J = 1.1$, Me–C(1)); 1.60 (*s*, Me–C(10)). ^{13}C-NMR (150 MHz, C_6D_6): 167.41 (*s*, MeO*C*O–C(5)); 167.31 (s, MeO*C*O–C(4)); 145.45 (*s*, C(6)); 143.83 (*s*, C(8)); 143.17 (*s*, C(1′)); 142.36 (*s*, C(1)); 138.96 (*d*, C(3)); 132.89 (*s*, C(5a)); 132.76 (*s*, C(4)); 130.97 (*s*, C(10)); 130.94 (*d*, C(9)); 128.70 (*s*, C(10a)); 128.65 (*d*, C(3′,5′)); 127.96 (*d*, C(7)); 127.87 (*d*, C(2′,6′)); 127.71 (*d*, C(4′)); 126.65 (*d*, C(2)); 123.84 (*s*, C(5)); 51.54 (*q*, *Me*OCO–C(5)); 51.52 (*q*, *Me*OCO–C(4)); 23.20 (*q, Me*–C(1)); 22.31 (*q, Me*–C(6)); 18.29 (*q, Me*–C(10)). EI-MS: 388.1 (100, $M^{+\cdot}$), 373.1 (20, $[M-Me]^+$), 341.1 (38, $[M-(Me+MeOH)]^+$), 297.0 (46, $[M-(MeOCO+MeOH)]^+$), 252.0 (40, $[M-(MeOCO+Ph)]^{+\cdot}$), 246.0 (75, $[M-ADM]^{+\cdot}$), 239.0 (64, $[M-(PhC{\equiv}CH+MeOH+Me)]^+$), 215.0 (29), 119.6 (34). Anal. calc. for $C_{25}H_{24}O_4$ (388.46): C 77.29, H 6.22; found: C 77.15, H 6.31.

The structure of **2d** was established by an X-ray crystal-structure analysis (*cf. Tables 3* and *5*).

2.6.2. *Tetramethyl* endo-*3a,6-Dihydro-1,6,9-trimethyl-7-phenyl-1,3a-methanophenalene-2,3,4,5-tetracarboxylate* (*endo*-**5d**)[12]. Yield 0.026 g (4%). Colorless crystals. M.p. 186–187° (hexane/CH_2Cl_2). R_f (hexane/Et_2O

1:1) 0.24. IR (KBr): 3064*w*, 3026*w*, 2972*w*, 1722*s*, 1643*w*, 1625*m*, 1442*m*, 1370*w*, 1325*m*, 1284*s*, 1263*s*, 1189*m*, 1103*s*, 1032*s*, 990*w*, 712*m*, 627*w*. ^{1}H-NMR (600 MHz, $CDCl_3$): 7.40 (*t*, $J_o = 7.4$, H–C(3′,5′)); 7.35 (*t*, $J_o = 7.4$, H–C(4′)); 7.31 (*dd*, $J_o = 7.5$, $J_m = 1.3$, H–C(2′,6′)); 6.68 (*s*, H–C(8)); 4.09 (*q*, $^3J = 7.1$, H–C(6)); 3.83 (*s*, MeOCO–C(4)); 3.81 (*s*, MeOCO–C(5)); 3.79 (*s*, MeOCO–C(2)); 3.67 (*s*, MeOCO–C(3)); 2.89 (*d*, $^2J = 7.4$, H_a–C(10)); 2.42 (*s*, Me–C(9)); 2.37 (*d*, $^2J = 7.4$, H_s–C(10)); 1.86 (*s*, Me–C(1)); 0.93 (*d*, $^3J = 7.1$, Me–C(6)). ^{13}C-NMR (150 MHz, $CDCl_3$): 169.52 (*s*, MeO*C*O–C(5)); 166.33 (*s*, MeO*C*O–C(4)); 165.77 (*s*, MeO*C*O–C(2)); 163.76 (*s*, MeO*C*O–C(3)); 154.00 (*s*, C(2)); 150.59 (*s*, C(3)); 146.69 (*s*, C(5)); 144.64 (*s*, C(9a)); 144.38 (*s*, C(9b)); 140.32 (*s*, C(1′)); 137.29 (*s*, C(9)); 131.21 (*d*, C(8)); 131.01 (*s*, C(7)); 128.76 (*s*, C(6a)); 128.74 (*d*, C(2′,6′)); 128.42 (*d*, C(3′,5′)); 128.21 (*s*, C(4)); 127.04 (*d*, C(4′)); 76.70 (*t*, C(10)); 59.36 (*s*, C(1)); 56.36 (*s*, C(3a)); 52.49 (*q*, *Me*OCO–C(5)); 52.17 (*q*, *Me*OCO–C(2)); 52.12 (*q*, *Me*OCO–C(4)); 51.69 (*q*, *Me*OCO–C(3)); 34.72 (*d*, C(6)); 20.31 (*q*, *Me*–C(6)); 18.22 (*q*, *Me*–C(9)); 16.12 (*q*, *Me*–C(1)). CI-MS: 548.2 (100, $[M + NH_4]^+$), 531.2 (19, $[M + H]^+$), 499.2 (9, $[(M + H) - MeOH]^+$), 386.2 (7), 330.2 (8), 286 (2). Anal. calc. for $C_{31}H_{30}O_8$ (530.57): C 70.17, H 5.69; found: C 69.91, H 5.77.

The structure of *endo*-**5d** was established by an X-ray crystal-structure analysis (*cf. Fig. 2* and *Table 5*).

2.6.3. *Tetramethyl* endo-*2,8,12-Trimethyl-10-phenyltetracyclo[6.4.1.1^{2,5}.0^{5,13}]tetradeca-1(13),3,6,9,11-pentaene-3,4,6,7-tetracarboxylate* (*endo*-**3d**)[12]. Trace amounts. Yellow spot on TLC; R_f (hexane/AcOEt 2:1) 0.34.

2.6.4. *Tetramethyl* exo-*2,8,12-Trimethyl-10-phenylpentacyclo[6.4.1.1^{2,5}.0^{5,13}.0^{9,13}]tetradeca-1(12),3,6,10-tetraene-3,4,6,7-tetracarboxylate* (*exo*-**4d**)[12]. Trace amounts. t_R (see *2.4*) 10.88 min. UV/VIS (hexane/i-PrOH 95:5): λ_{max} 355 (0.32), 265 (0.60), 206 (1.00); λ_{min} 310 (0.22), 240 (0.49).

2.6.5. *Tetramethyl* trans-*2,4a-Dihydro-3,8,9-trimethyl-6-phenylphenanthrene-1,2,4,4a-tetracarboxylate* (*trans*-**6d**)[12]. Trace amounts. t_R (see above) 11.66 min. UV/VIS (hexane/i-PrOH 95:5): λ_{max} 340 (0.27), 260 (0.61), 207 (1.00); λ_{min} 310 (0.22), 240 (0.48).

2.6.6. *Dimethyl 4,8-Dimethyl-6-phenylazulene-1,2-dicarboxylate* (**11d**). Trace amounts. Blue spot on TLC. R_f (hexane/AcOEt 2:1) 0.42. t_R (see *2.4*) 5.88 min. UV/VIS (hexane/i-PrOH 95:5): λ_{max} 378 (0.28), 312 (1.00), 255 (0.49); λ_{min} 335 (0.23), 270 (0.30).

2.6.7. *Dimethyl (Z)-1-(1,4,8-Trimethyl-6-phenylazulen-3-yl)ethene-1,2-dicarboxylate* ((*Z*)-**10d**). Trace amounts. t_R (see *2.4*) 6.18 min. UV/VIS (hexane/i-PrOH 95:5): λ_{max} 380 (0.15), 326 (sh, 0.39), 276 (1.00), 250 (sh, 0.72), 205 (0.67); λ_{min} 360 (0.14), 315 (0.38), 220 (0.51).

2.7. *Reaction of 6-(3,5-Dimethylphenyl)-1,4,8-trimethylazulene* (**1e**). A soln. of the azulene (0.220 g, 0.80 mmol) and ADM (0.3 ml, 2.40 mmol) in toluene (10 ml) was degassed with Ar and heated in a closed 50-ml *Schlenk* vessel at 130° for 24 h. The solvent was distilled off, and the residue was subjected to CC (silica gel; hexane/Et_2O 1:2) to give **2e**.

2.7.1. *Dimethyl 8-(3,5-Dimethylphenyl)-1,6,10-trimethylheptalene-4,5-dicarboxylate* (**2e**). Yield 0.082 g (12%). Yellow crystals. M.p. 154–155°. R_f (hexane/Et_2O 1:1) 0.46. UV/VIS: see *Table 4* and *Fig. 11*. ^{1}H-NMR (300 MHz, $CDCl_3$): 7.55 (*d*, $^3J = 5.9$, H–C(3)); 7.08 (br. *s*, H–C(2′,6′)); 6.94 (*d*, H–C(4′)); 6.61 (*s*, H–C(7)); 6.32 (br. *d*, $^3J = 5.9$, H–C(2)); 6.30 (*s*, H–C(9)); 3.73 (*s*, MeOCO–C(5)); 3.69 (*s*, MeOCO–C(4)); 2.35 (*s*, Me–C(3′,5′)); 2.06 (*d*, $^4J \approx 1.5$, Me–C(1)); 2.05 (*s*, Me–C(6)); 1.86 (*s*, Me–C(10)).

2.8. *Reaction of 6-(1,1′-Biphenyl-4-yl)-1,4,8-trimethylazulene* (**1f**). A soln. of the azulene (0.200 g, 0.62 mmol) and ADM (0.23 ml, 1.86 mmol) in MeCN (10 ml) was degassed with Ar and heated in a closed 50-ml *Schlenk* vessel at 130° for 24 h. The solvent was distilled off, and the residue was subjected to CC (silica gel; hexane/Et_2O 1:2). The following seven products were isolated.

2.8.1. *Dimethyl 8-(1,1′-Biphenyl-4-yl)-1,6,10-trimethylheptalene-4,5-dicarboxylate* (**2f**). Yield 0.100 g (35%). Yellow crystals. M.p. 203–204° (Et_2O/CH_2Cl_2). R_f (hexane /Et_2O 1:1) 0.44. UV/VIS: see *Table 4* and *Fig. 12*. IR (KBr): 3427*w*, 2987*m*, 1716*s*, 1643*w*, 1599*w*, 1560*w*, 1486*m*, 1375*w*, 1256*s*, 1195*m*, 1053*s*, 884*m*, 769*s*. ^{1}H-NMR (300 MHz, C_6D_6): 7.74 (*dq*-like, $^3J = 5.9$, $^5J = 0.9$, H–C(3)); 7.54–7.45 (*m*, H–C(2′,3′,5′,6′), H–C(2″,6″)); 7.24 (*t*, $J_o = 7.6$, H–C(3″,5″)), 7.16 (*tt*, $J_o = 7.3$, $J_m = 1.2$, H–C(4″)); 6.63 (*s*, H–C(9)); 6.43 (*quint*, $J = 1.3$, H–C(7)); 5.91 (*dq*-like, $^3J = 5.9$, $^4J = 1.4$, H–C(2)); 3.48 (*s*, MeOCO–C(5)); 3.26 (*s*, MeOCO–C(4)); 2.06 (*d*, $^4J = 1.2$, Me–C(6)); 1.77 (*d*-like, $J = 0.9$, Me–C(1)); 1.64 (*s*, Me–C(10)). ^{1}H-NMR (600 MHz, $CDCl_3$): 7.62 (*dd*, $J_o = 8.2$, $J_m = 1.2$, H–C(2″,6″); 7.602, 7.570 (AA′BB′, $J_{AB} = 8.3$, H–C(3′,5′), H–C(2′,6′), resp.); 7.567 (*dd*, $^3J \approx 6$, $^5J \approx 0.8$, H–C(3)); 7.45 (*t*, $J_o = 7.7$, H–C(3″,5″)); 7.36 (*tt*, $J_o = 7.4$, $J_m = 1.2$, H–C(4″)); 6.72 (*s*, H–C(9)); 6.38 (*quint*-like, $^4J = 1.3$, H–C(7)); 6.34 (*dq*-like, $^3J = 6.0$, $^4J = 1.4$, H–C(2)); 3.75 (*s*, MeOCO–C(5)); 3.70 (*s*, MeOCO–C(4)); 2.09 (*t*, superpos. of Me–C(1), Me–C(6)); 1.89 (*s*, Me–C(10)). ^{13}C-NMR (150 MHz, $CDCl_3$): 167.67 (*s*, MeO*C*O–C(5)); 167.47 (*s*, MeO*C*O–C(4)); 145.07 (*s*, C(6)); 142.76 (*s*, C(1)); 142.53 (*s*, C(8)); 141.46 (*s*, C(1′)); 140.75 (*s*, C(1″)); 140.19 (*s*, C(4′)); 139.13 (*s*, C(3)); 132.54 (*s*, C(5a)); 131.36 (*s*, C(4)); 130.77 (*s*, C(10)); 130.40 (*d*, C(9)); 128.75 (*d*, C(3″,5″)); 128.38 (*s*, C(10a)); 127.49 (*d*, C(3′,5′));

Table 5. *Crystallographic Data for Compounds* **2a**, **2d**, **2f**, exo-**4a**, endo-**5d**, trans-**6a**, *[1-^{2}H]*-**7a**, syn-*[11-^{2}H]*-**8a**, *and [1-^{2}H]*-**9**

	2a	**2d**	**2f**	*exo*-**4a**
Crystallized from	Et_2O/hexane	Et_2O/hexane	Et_2O/CH_2Cl_2	hexane/CH_2Cl_2
Empirical formula	$C_{23}H_{28}O_4$	$C_{25}H_{24}O_4$	$C_{31}H_{28}O_4$	$C_{29}H_{34}O_8$
Formula weight [g mol^{-1}]	368.47	388.46	464.56	510.58
Crystal color, habit	yellow, prism	yellow, prism	yellow, prism	colorless, plate
Crystal dimensions [mm]	$0.25 \times 0.30 \times 0.30$	$0.23 \times 0.23 \times 0.45$	$0.35 \times 0.45 \times 0.50$	$0.12 \times 0.38 \times 0.40$
Diffractometer	*Nonius Kappa CCD*	*Rigaku AFC5R*	*Rigaku AFC5R*	*Rigaku AFC5R*
Temperature [K]	160(1)	173(1)	173(1)	173(1)
Crystal system	monoclinic	triclinic	monoclinic	orthorhombic
Space group	$P2_1/n$	$P\bar{1}$	$P2_1/c$	*Pbca*
Z	4	2	4	8
Reflections for cell determination	6102	25	25	18
2θ Range for cell determination [°]	4 – 60	38 – 40	36 – 40	20 – 32
Unit-cell parameters a [Å]	6.3426(1)	10.988(1)	15.372(3)	15.798(5)
b [Å]	17.8736(2)	13.598(1)	11.973(6)	36.388(7)
c [Å]	18.1665(3)	6.8476(6)	14.359(3)	9.425(7)
α [°]	90	97.402(6)	90	90
β [°]	98.4775(5)	97.875(7)	110.30(1)	90
γ [°]	90	93.608(7)	90	90
V [Å^3]	2036.95(5)	1001.7(2)	2479(1)	5418(4)
$F(000)$	792	412	984	2176
D_x [g cm^{-3}]	1.201	1.288	1.245	1.252
μ (MoK_α) [mm^{-1}]	0.0808	0.0862	0.0812	0.0906
Scan type	ϕ and ω	$\omega/2\theta$	$\omega/2\theta$	ω
$2\theta_{(max)}$ [°]	60	55	55	55
Total reflections measured	57887	4830	6184	7957
Symmetry independent reflections	5923	4591	5679	6217
R_{int}	0.047	0.015	0.026	0.044
Reflections used [$I > 2\sigma(I)$]	4388	3611	3319	3171
Parameters refined	245	263	317	335
Final $R(F)$	0.0553	0.0434	0.0497	0.0541
$wR(F)$	0.0564	0.0434	0.0412	0.0433
Weights: p in $w = [\sigma^2(F_o) + (pF_o)^2]^{-1}$	0.005	0.005	0.005	0.005
Goodness-of-fit	3.425	2.130	1.730	1.496
Secondary extinction coefficient	$2.6(4) \times 10^{-6}$	$2.1(2) \times 10^{-6}$	$4.0(5) \times 10^{-7}$	$4(1) \times 10^{-8}$
Final Δ_{max}/σ	0.0007	0.0003	0.0003	0.0002
$\Delta\rho$(max; min) [e Å^{-3}]	0.40; −0.28	0.32; −0.25	0.53; −0.21	0.29; −0.28
Structure solution program	SIR922 [39]	SIR92	SIR92	SHELXS97 [40]

127.25 (*d*, C(4″)); 127.03 (*d,* C(2′,6′)); 127.00 (*d*, C(2″,6″)); 126.94 (*d*, C(7)); 126.20 (d, C(2)); 122.68 (*s*, C(5)); 52.03 (*q*, *Me*OCO−C(5)); 51.97 (*q*, *Me*OCO−C(4)); 23.37 (*q*, *Me*−C(1)); 22.28 (*q*, *Me*−C(6)); 18.47 (*q*, *Me*−C(10)). CI-MS: 482.1 (100, $[M + NH_4]^+$), 465.1(8, $[M + H]^+$), 460.0 (2). Anal. calc. for $C_{31}H_{28}O_4$ (464.56): C 80.14, H 6.07; found: C 79.73, H 6.14.

The structure **2f** was established by X-ray crystal-structure analysis (*cf. Fig. 8*, and *Tables 3* and *5*).

2.8.2. *Tetramethyl* endo-*7-(1,1′-Biphenyl-4-yl)-3a,6-dihydro-1,6,9-trimethyl-1,3a-methanophenalene-2,3,4,5-tetracarboxylate* (*endo*-**5f**)[12]). Trace amounts in a chromatographic fraction. Identified by some of its characteristic ^{1}H-NMR signals (300 MHz, $CDCl_3$): 6.73 (*s*, H−C(8)); 4.15 (*q*, $^3J = 7.1$, H−C(6)); 2.90 (*d*, $^2J = 7.4$, H_a−C(10)); 2.44 (*s*, Me−C(9)); *ca.* 2.40 (*d*, H_s−C(10)); 1.87 (*s*, Me−C(1)); 0.98 (*d*, $^3J = 7.1$, Me−C(6)).

endo-**5d**	*trans*-**6a**	*[1-^{2}H]*-**7a**	*syn-[11-^{2}H]*-**8a**	*[1-^{2}H]*-**9**
hexane/CH_2Cl_2	Et_2O/CH_2Cl_2	Et_2O/CH_2Cl_2	Et_2O	Et_2O
$C_{31}H_{30}O_8$	$C_{29}H_{34}O_8$	$C_{29}H_{34}O_8$	$C_{29}H_{34}O_8$	$C_{20}H_{20}O_8$
530.57	510.58	510.58	510.58	388.37
colorless, prism	pale green, plate	colorless, needle	pale yellow, plate	pale blue, plate
$0.23 \times 0.45 \times 0.55$	$0.10 \times 0.28 \times 0.43$	$0.05 \times 0.10 \times 0.25$	$0.05 \times 0.12 \times 0.30$	$0.02 \times 0.25 \times 0.25$
Rigaku AFC5R	*Rigaku AFC5R*	*Nonius Kappa CCD*	*Nonius Kappa CCD*	*Nonius Kappa CCD*
173(1)	173(1)	160(1)	160(1)	160(1)
monoclinic	monoclinic	triclinic	triclinic	monoclinic
$P2_1$	$P2_1/n$	$P\bar{1}$	$P\bar{1}$	$P2_1/c$
2	4	2	2	4
25	25	4673	6061	4412
38 – 40	20 – 37	2 – 50	2 – 55	2 – 55
7.853(4)	11.631(3)	9.4404(2)	8.1494(1)	10.1890(2)
16.234(4)	16.196(4)	12.0217(3)	11.6786(2)	8.9606(2)
10.534(2)	14.671(4)	13.3792(4)	15.3519(3)	20.0821(4)
90	90	108.7666(9)	74.8621(7)	90
93.12(3)	110.16(2)	100.4777(9)	77.5788(7)	94.3662(9)
90	90	104.259(1)	71.3277(9)	90
1340.9(7)	2594(1)	1335.80(6)	1322.28(4)	1828.17(7)
560	1088	544	544	816
1.314	1.307	1.269	1.282	1.410
0.0946	0.0946	0.0919	0.0928	0.110
$\omega/2\theta$	$\omega/2\theta$	ω	ϕ and ω	ϕ and ω
60	50	50	55	54
4298	5003	27320	46405	33460
4029	4571	4675	6072	3983
0.021	0.058	0.072	0.051	0.042
3565	2351	3371	4572	3179
352	335	335	335	254
0.0389	0.0568	0.0472	0.0474	0.0441
0.0370	0.0442	0.0478	0.0520	0.0435
0.005	0.005	0.005	0.010	0.005
1.709	1.596	1.781	2.181	2.604
$2.6(2) \times 10^{-6}$	$2.0(4) \times 10^{-7}$	$2.5(3) \times 10^{-6}$	$2.9(4) \times 10^{-6}$	$1.3(2) \times 10^{-6}$
0.0005	0.00007	0.0002	0.0003	0.0002
0.28; – 0.23	0.29; – 0.26	0.23; – 0.26	0.28; – 0.27	0.25; – 0.26
SHELXS97	SIR9	SIR92	SHELXS97	SHELXS97

2.8.3. *Tetramethyl* exo-*10-(1,1′-Biphenyl-4-yl)-2,8,12-trimethylpentacyclo[6.4.1.1^{2,5}.0^{5,13}.0^{9,13}]tetradeca-1(12),3,6,10-tetraene-3,4,6,7-tetracarboxylate* (*exo*-**4f**)[12]. Trace amounts. t_R (see *2.4.*) 10.90 min. UV/VIS (hexane/i-PrOH 95 : 5): λ_{max} 315 (0.35), 251 (0.79), 206 (1.00); λ_{min} 300 (0.31), 225 (0.62).

2.8.4. *Tetramethyl* trans-*6-(1,1′-Biphenyl-4-yl)-2,4a-dihydro-3,8,9-trimethylphenanthrene-1,2,4,4a-tetracarboxylate* (*trans*-**6f**)[12]. Trace amounts. t_R (see *2.4*) 10.14 min. UV/VIS (hexane/i-PrOH 95 : 5): λ_{max} 323 (0.39), 247 (0.54), 206 (1.00); λ_{min} 298 (0.33), 230 (0.52).

2.8.5. *Tetramethyl* endo-*10-(1,1′-Biphenyl-4-yl)-2,8,12-trimethyltetracyclo[6.4.1.1^{2,5}.0^{5,13}]tetradeca-1(13),3,6,9,11-pentaene-3,4,6,7-tetracarboxylate* (*endo*-**3f**)[12]. Trace amounts. Yellow spot on TLC: R_f (hexane/AcOEt 2 : 1) 0.34.

2.8.6. *Dimethyl 6-(1,1′-biphenyl-4-yl)-4,8-dimethylazulene-1,2-dicarboxylate* (**11f**). Trace amounts. Blue spot on TLC: R_f (hexane/AcOEt 2 : 1) 0.43.

2.8.7. *Dimethyl (Z)-1-[6-((1,1′-Biphenyl-4-yl)-1,3,4,8-trimethylazulen-3-yl]ethene-1,2-dicarboxylate* ((*Z*)-**10f**). Trace amounts. t_R (see *2.4.*) 10.14 min. UV/VIS (hexane/i-PrOH 95 : 5): λ_{max} 372 (sh, 0.32), 315 (sh, 0.44), 300 (0.52), 260 (0.67), 206 (1.00); λ_{min} 345 (0.37), 270 (0.52), 242 (0.55).

3. X-Ray Crystal-Structure Determinations of Compounds 2a, 2d, 2f, *exo*-4a, *endo*-5d, *trans*-6a, [1-^{2}H]-7a, *syn*-[11-^{2}H]-8a, and [1-^{2}H]-9[15]). – All measurements were conducted at low temp. with graphite-monochromated MoK_α radiation ($\lambda = 0.71073$ Å). The data collection and refinement parameters are given in *Table 5* and views of the molecules are shown in *Figs. 1*, *2*, and *4–8*. The intensities were corrected for *Lorentz* and polarization effects, and for **2f**, an empirical absorption correction, based on azimuthal scans of several reflections [31], was also applied (transmission factors: $T_{min} = 0.918$; $T_{max} = 0.972$). Equivalent reflections were merged, except for *Friedel* pairs in the case of *endo*-**5d**. Each structure was solved by direct methods, which revealed the positions of all non-H-atoms, and the non-H-atoms were refined anisotropically. All of the H-atoms were fixed in geometrically calculated positions (d(C–H) = 0.95 Å), and each was assigned a fixed isotropic displacement parameter with a value equal to $1.2U_{eq}$ of its parent C-atom. Refinement of each structure was carried out on F by full-matrix least-squares procedures, which minimized the function $\Sigma w(|F_o| - |F_c|)^2$. Corrections for secondary extinction were applied. For **2a**, [1-^{2}H]-**7a**, *syn*-[11-^{2}H]-**8a**, and [1-^{2}H]-**9**, four, six, one, and five reflections, resp., whose intensities were considered to be extreme outliers, were omitted from the final refinement. The crystals of *endo*-**5d** were either enantiomerically pure or racemic twins, but the absolute configuration was not determined because of the low anomalous scattering power of the compound. Instead, the direction of the polar axis was chosen arbitrarily.

Neutral-atom-scattering factors for non-H-atoms were taken from [32], and the scattering factors for H-atoms were taken from [33]. Anomalous dispersion effects were included in F_{calc} [34]; the values for f' and f'' were those from [35]. The values of the mass-attenuation coefficients were taken from [36]. All calculations were performed with the teXsan crystallographic software package [37] and the crystallographic diagrams were drawn using ORTEPII [38].

REFERENCES

[1] a) K. Hafner, H. Diehl, H. U. Süss, *Angew. Chem.* **1976**, *88*, 121; *Angew. Chem., Int. Ed.* **1976**, *15*, 104; b) K. Hafner, G. L. Knaup, H. J. Lindner, *Bull. Soc. Chem. Jpn.* **1988**, *61*, 155.
[2] Y. Chen, R. W. Kunz, P. Uebelhart, R. H. Weber, H.-J. Hansen, *Helv. Chim. Acta* **1992**, *75*, 2447.
[3] a) S. El Houar, H.-J. Hansen, *Helv. Chim. Acta* **1997**, *80*, 253; b) M. Lutz, A. Linden, K. Abou-Hadeed, H.-J. Hansen, *Helv. Chim. Acta* **1999**, *82*, 372.
[4] P. Uebelhart, H.-J. Hansen, *Helv. Chim. Acta* **1992**, *75*, 2493; Y. Chen, H.-J. Hansen, *Helv. Chim. Acta* **1993**, *76*, 168.
[5] R.-A. Fallahpour, H.-J. Hansen, *High Pressure Res.* **1992**, *11*, 125, and *Helv. Chim. Acta* **1995**, *78*, 1933.
[6] J. Guspanová, R. Knecht, M. Laganà, C. Weymuth, H.-J. Hansen, *Helv. Chim. Acta* **1997**, *80*, 1375.
[7] A. A. S. Briquet, P. Uebelhart, H.-J. Hansen, *Helv. Chim. Acta* **1996**, *79*, 2282.
[8] J. Song, H.-J. Hansen, *Helv. Chim. Acta* **1999**, *82*, 1690 and 2260.
[9] W. Bernhard, H.-R. Zumbrunnen, H.-J. Hansen, *Chimia* **1979**, *33*, 324.
[10] K. Hafner, H. Kaiser, *Liebigs Ann. Chem.* **1958**, *618*, 140, and *Org. Synth., Coll. Vol.* **1973**, *5*, 1088.
[11] P. Brügger, P. Uebelhart, R. W. Kunz, R. Sigrist, H.-J. Hansen, *Helv. Chim. Acta* **1998**, *81*, 2201.
[12] A. Magnussen, H.-J. Hansen, *Helv. Chim. Acta* **1997**, *80*, 545.
[13] A. Linden, M. Meyer, P. Mohler, A. J. Rippert, H.-J. Hansen, *Helv. Chim. Acta* **1999**, *82*, 2274.
[14] W. T. Ford, *J. Org. Chem.* **1971**, *36*, 3979.
[15] S. McLean, C. J. Webster, R. J. D. Rutherford, *Can. J. Chem.* **1969**, *47*, 1555.
[16] V. Lellek, H.-J. Hansen, *Helv. Chim. Acta* **2001**, *84*, 1712.
[17] M. T. Reetz, *Angew. Chem.* **1972**, *84*, 163; *Angew. Chem., Int. Ed.* **1972**, *11*, 130.
[18] M. T. Reetz, *Angew. Chem.* **1972**, *84*, 161; *Angew. Chem., Int. Ed.* **1972**, *11*, 129.
[19] M. T. Reetz, *Chem. Ber.* **1977**, *110*, 954 and 965; M. T. Reetz, N. Greif, *Angew. Chem.* **1977**, *89*, 765; *Angew. Chem., Int. Ed.* **1977**, *16*, 712.

---

[15]) Crystallographic date (excluding structure factors) for the structures of **2a**, **2d**, **2f**, *exo*-**4a**, *endo*-**5d**, *trans*-**6a**, [1-^{2}H]-**7a**, *syn*-[11-^{2}H]-**8a**, and [1-^{2}H]-**9** have been deposited with the *Cambridge Crystallographic Data Centre* as supplementary publications No. CCDC-169387 to CCDC-169395, resp. Copies of the data can be obtained, free of charge, on application to the CCDC, 12 Union Road, Cambridge CB2 1EZ, UK (fax: +44-(0)1223-336033; e-mail: deposit@ccdc.cam.ac.uk).

[20] T. H. Black, W. J. DuBay III; P. S. Tully, *J. Org. Chem*. **1988**, *53*, 522; M. T. Reetz, A. Schmitz, X. Holdgrün, *Tetrahedron Lett*. **1989**, *40*, 5421; J. Mulzer, K. Hoyer, A. Müller-Fahrnow, *Angew. Chem.* **1997**, *109*, 1546; *Angew. Chem., Int. Ed.* **1997**, *36*, 1476.
[21] R. B. Woodward, R. Hoffmann, *Angew. Chem.* **1969**, *81*, 797; *Angew. Chem., Int. Ed.* **1969**, *8*, 781; N. T. Anh, 'Die Woodward-Hoffmann-Regeln und ihre Anwendung', VCH, Weinheim, 1972.
[22] K. Mackenzie, K. B. Astin, E. C. Gravett, R. J. Gregorry, J. A. K. Howard, C. Wilson, *J. Phys. Org. Chem*. **1998**, *11*, 879; W. Grimme, K. Pohl, J. Wortmann, D. Frowein, *Liebigs Ann Chem*. **1996**, 1905; K. N. Houk, Y. Li, M. A MacAllister, G. O'Doherty, L. A. Paquette, W. Siebbrand, Z. K. Smedarchina, *J. Am. Chem. Soc*. **1994**, *116*, 10895.
[23] C. W. Spangler, *Chem. Rev.* **1976**, *76*, 187.
[24] P. Uebelhard, H.-J. Hansen, unpublished results.
[25] A. P. Marchand, 'Stereochemical Applications of NMR Studies in Rigid Bicyclic Systems', Verlag Chemie International, Inc., Deerfield Beach, Florida, 1982.
[26] W. Bernhard, P. Brügger, P. Schönholzer, R. H. Weber, H.-J. Hansen, *Helv. Chim. Acta* **1985**, *68*, 429.
[27] K. Abou-Hadeed, H.-J. Hansen, *Helv. Chim. Acta* **1997**, *80*, 2535.
[28] W. Bernhard, P. Brügger, J. J. Daly, P. Schönholzer, R. H. Weber, H.-J. Hansen, *Helv. Chim. Acta* **1985**, *68*, 415.
[29] D. M. Ketcha, G. W. Gribble, *J. Org. Chem.* **1985**, *50*, 5455.
[30] J. Song, H.-J. Hansen, *Helv. Chim. Acta* **1999**, *82*, 309.
[31] A. C. T. North, D. C. Phillips, F. S. Mathews, *Acta Crystallogr. Sect. A* **1968**, *24*, 351.
[32] a) E. N. Maslen, A. G. Fox, M. A. O'Keefe, in 'International Tables for Crystallography', Ed. A. J. C. Wilson, Kluwer Academic Publishers, Dordrecht, 1992 Vol. C, Table 6.1.1.1, pp. 477–486.
[33] R. F. Stewart, E. R. Davidson, W. T. Simpson, *J. Chem. Phys.* **1965**, *42*, 3175.
[34] J. A. Ibers, W. C. Hamilton, *Acta Crystallogr.* **1964**, *17*, 781.
[35] D. C. Creagh, W. J. McAuley, in 'International Tables for Crystallography', Ed. A. J. C. Wilson, Kluwer Academic Publishers, Dordrecht, 1992 Vol. C, Table 4.2.6.8, pp. 219–222.
[36] D. C. Creagh, J. H. Hubbell, in 'International Tables for Crystallography', Ed. A. J. C. Wilson, Kluwer Academic Publishers, Dordrecht, 1992 Vol. C, Table 4.2.4.3, pp. 200–206.
[37] teXsan: Single Crystal Structure Analysis Software, Version 1.10, Molecular Structure Corporation, The Woodlands, Texas, 1999.
[38] C. K. Johnson, ORTEPII, Report ORNL-5138, Oak Ridge National Laboratory, Oak Ridge, Tennessee, 1976.
[39] A. Altomare, G. Cascarano, C. Giacovazzo, A. Guagliardi, M. C. Burla, G. Polidori, M. Camalli, *SIR92*, *J. Appl. Crystallogr.* **1994**, *27*, 435.
[40] G. M. Sheldrick, SHELXS97, 'Program for the Solution of Crystal Structures', University of Göttingen, Germany, 1997.

Received May 25, 2001